Analyst

Accepted Manuscript

This article can be cited before page numbers have been issued, to do this please use: A. Qureshi and J. H. Niazi, *Analyst*, 2020, DOI: 10.1039/D0AN00896F.

ROYAL SOCIETY OF CHEMISTRY

rsc.li/analyst

View Article Online
DOI: 10.1039/D0AN00896F

Biosensors for detecting viral and bacterial infections using host biomarkers: a review

Anjum Qureshi* and Javed H. Niazi*

Sabanci University, SUNUM Nanotechnology Research and Application Center, Tuzla 34956, Istanbul, Turkey

*Corresponding authors email: anjum@sabanciuniv.edu; javed@sabanciuniv.edu
Tel: +90 216 483 2441/9879

View Article Online
DOI: 10.1039/D0AN00896F

Abstract

Viral and bacterial infections commonly occur by their transmission through air, contaminated food, water, body fluids or physical contact between person to person. They rapidly spread among the population causing millions of deaths worldwide. One of the major challenges in the diagnosis of infection is to differentially diagnose viral from bacterial infections. Constant viral mutations, reassortment and recombination give rise to emergence of new and diverse viral populations which makes it difficult for diagnosis. Antibiotics prescribed for patients suffering from viral infections are ineffective and a contributing factor to bacterial antibiotic resistance. Evaluating existing biosensing platforms for early diagnosis of bacterial etiology of infections enables researchers and clinicians to differentially diagnose viral infections. Over the last decade, many biosensors have been developed to detect a wide range of bacterial and viral markers and reduce the costs for healthcare. There has been considerable interest in finding diagnostic and prognostic biomarkers that can be detected in blood and predict the bacterial and viral infections. This review provides an overview on existing biosensor technology platforms for host biomarkers detection that can be applied for differentially diagnosing viral and bacterial infections, as well as considerations recommended and future prospects of viral/bacterial infection detection technology.

Keywords: Virus, bacteria, infection, point-of-care, biosensor, electrochemical, optical, microfluidics, diagnosis

1. Introduction

Infectious diseases are disorders that are caused by pathogenic organisms, which are microscopic in their dimensions, such as bacteria (~0.5–10 μm), viruses (~50–200 nm), parasites or fungi (~5–100 μm) and directly or indirectly can be transmitted from one person to another through contact, contaminated air, water or food.[1] Some of the most common infectious diseases include lower respiratory infections, diarrheal, influenza, tuberculosis, HIV/AIDS, malaria and hepatitis. According to latest World Health Organization (WHO) report, three infectious diseases ranked among the top ten causes of death worldwide in 2016, such as lower respiratory infections (3.0 million deaths), diarrheal diseases (1.4 million deaths) and tuberculosis (1.3 million deaths).[2] Diagnostic uncertainty and inaccurate diagnosis in distinguishing bacterial/viral infections especially related to Lower Respiratory Tract Infections (LRTIs) is one of the major factors for disease outbreak. According to a recent WHO Global Influenza Surveillance and Response System (GISRS), influenza A(H1N1) subtype strain is more frequent type of viral infections recorded during 2019-2020[3] (Fig. 1) and reached a highest peak in the current year 2020.

View Article Online
DOI: 10.1039/D0AN00896F

Recent coronavirus 2019 (COVID-19) pandemic outbreak first reported from Wuhan, China in December 2019 has caused nearly 700 thousands deaths and confirmed over 17 million positive cases according to WHO.[4] Infectious diseases are generally confined to specific places, for instance, Wuhan in China for COVID-19 and transmitted from one person to another through global traveling/transportation, water, sanitation, food and climate that possessed risk of recently reported pathogen outbreaks.[5-10]

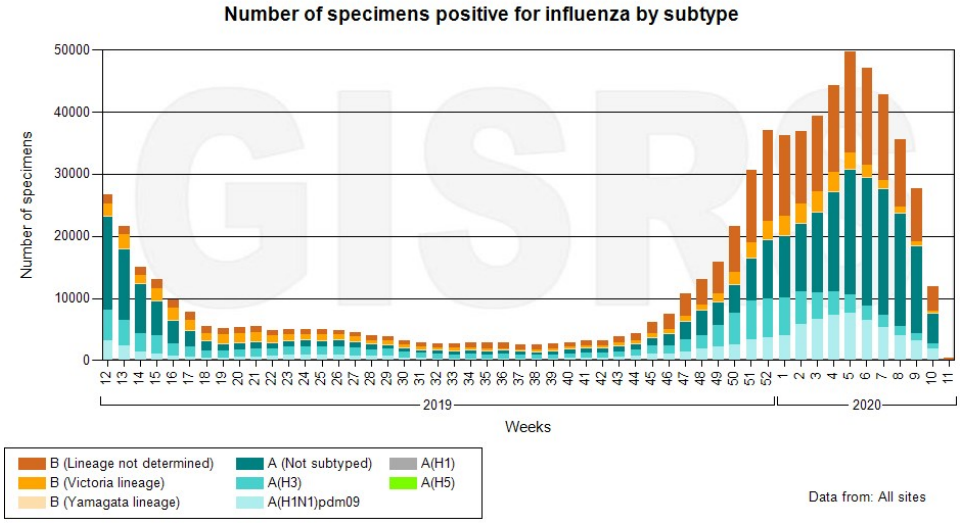

Fig. 1. Profile of influenza virus subtypes in global circulation of influenza types detected based on the order of highest to lowest number of incidence are; influenza A and B (no subtype lineage identified) followed by influenza A subtypes (H1N1), (H3) and B-Yamagata subtype.

Unnecessary use of antibiotics as a consequence of disease outbreak may further trigger widespread antibiotic resistance. Excessive use of antibiotics is a major issue worldwide in many developing countries, where most antibiotics can be accessed over the counter. According to a latest WHO report, antibiotic resistance and susceptibility is reported to be higher in Belgium, Cyprus, France, Greece, Romania, Serbia and Turkey among the European countries (Fig. S1).[11] Therefore, identifying the infection type becomes a necessity using several alternative approaches, such as by screening for elevated blood levels of causative bacterial and/or viral antibodies, specific biomarkers or nucleic acid sequences. Existing methods rely on expensive DNA/RNA-based detection of virus from samples, such as quantitative real-time reverse transcriptase polymerase chain reaction (RT-qPCR). These nucleic acids-based detection methods are although sensitive, but they heavily rely on time-consuming isolation and complicated sample pre-processing. Therefore, there is an urgent demand for novel, simple and cost-efficient diagnostic technologies to assist healthcare professionals in making more convenient point-of

View Article Online
DOI: 10.1039/D0AN00896F

care (PoC) clinical decisions for early detection of infectious viral/bacterial diseases that pave way to preventing disease transmission, secure public health and provide early diagnosis and treatment.

Extension of existing biosensors to PoC platforms could be promising in solving some of the major problems concerning early detection, speed, sensitivity and cost of measurements.[16] WHO has provided guidance for selection of a diagnostic test with benchmark criteria of ASSURED (Affordable, Sensitive, Specific, User-Friendly, Robust and rapid, Equipment free, Deliverable) that can help in rapid diagnosis, providing better healthcare and reducing the waiting time and cost for results dissemination.[17] Recently, current state-of-the-art biosensor technologies developed for the infectious diseases detection has been reviewed that utilized cell-phone, magnetic barcode, lab-on-a chip and microfluidics platforms.[18, 19] These previously reported reviews provided information on a few commercially available PoC immunosensing instruments and optical, electrochemical, magnetic, and colorimetric based biosensor technologies for detection of viral and bacterial pathogens, such as such as human immunodeficiency virus (HIV), hepatitis B virus (HBV), and hepatitis C virus (HCV), Mycobacterium tuberculosis (MTB), *Plasmodium* species (malaria), Dengue, Zika, Chikungunya, non-structural (NS1) protein of influenza A viruses, Influenza (H5N1), Influenza (H1N1), *E. coli* O157:H7, *V. cholera* O1, *S. mutans* and *P. aeruginosa*.[18, 19]

In the present review, we explored some of the existing biosensing technologies that addressed detection of key host biomarkers that can serve as signatures of viral or bacterial infections for differential diagnosis. The review highlights the developments taken place over the past 5 years in biosensing technology toward biomarkers detection from bacterial/viral related Respiratory Tract Infections (RTIs) and risk assessments. The review also summarized frequently targeted biomarkers in differentiating or predicting bacterial and viral infections with their detection limit/range and bioassay designs. Finally, the review ends with a brief note on future prospects of detecting viral infections and possible means by which pandemics such as the recent COVID-19 can be prevented.

2. Conventional methods used for diagnosis of RTIs

There are diverse pathogens involved in upper and lower respiratory tract infections (Table S1 and Fig. S2). Other causes of RTIs are smoking, exposure of dust, chemicals vapors, fumes, allergens and air pollution.[22]

Serological identification or immunological identification of antigens or antibodies are standard conventional methods that provide early RTI diagnosis for uncultivable organisms in laboratory settings. Conventional serological methods include precipitation, agglutination, hemagglutination or its inhibition, complement fixation test and fluorescent antibody test and their specific features are summarized in Figure 2.[23, 24] Many of these classical methods are limited to accessible infections, such as microscopy and microorganism culturing since they are based on examining clinical samples taken from the infected

View Article Online
DOI: 10.1039/D0AN00896F

site of the patient and are expensive and futile for inaccessible infections. Most sensitive diagnostic approaches rely on host biomarker detection, such as Enzyme-Linked Immunosorbent Assay (ELISA) require laborious washing steps in order to separate unbound analyte and labeling free ligands/receptors to minimize the non-specific fluorescent background signal and complex matrix susceptibility. Infectious diseases can be successfully detected using ELISA-like immunoassays for host biomarker detections provided that antibody–antigen (biomarker) pair are correctly chosen but are difficult for detecting pathogens with high rates of mutation, such as in viruses, which affect the stability and structure of target probe biomolecule or specificity and weaken the sensitivity of immunoassay platform. Isolating and culturing of microbes is a time-consuming process, which requires multiple days to weeks to yield results, during this time the infection could advance within the patient and become contagious throughout the population. This prompts physicians to experimentally recommend antibiotics, while pending results of bacterial/viral culture to arrive, which risks prevalence of antibiotic resistant bacteria.[13] Microscopy is although more efficient with respect to time, but it is limited in scope for inaccessible infections and PoC applications.[25] Therefore, existing conventional diagnostic approaches are more prone to error and not suitable for inaccessible infections nor applicable in remote places, where infectious diseases maybe be more prevalent.[26]

The standard and diagnosis technique to date for detection of inaccessible infection derived from pathogenic virus and bacteria are nucleic acid-based assays, such as reverse transcriptase quantitative PCR (RT-qPCR) and DNA microarrays. These nucleic acid-based assays target specific DNA/RNA sequences extracted from microorganisms in clinical samples, amplify these sequences using specific probes and quantitatively detect copies of amplified sequences for accurate diagnosis of bacterial/viral infections. However, these assays demand expensive laboratory equipment, reagents or assay kits and required highly trained professionals to run the tests.[27, 28] Unfortunately, there are many regions around the world where such technical approaches simply are unsustainable. Therefore, collecting and transporting biological samples to the nearest clinical laboratory facility or hospital capable of performing such procedures has become a common practice. Further, reaching the results to physician could take several days to a week time, only then the physician could begin proper treatment. Situations such as during the disease outbreaks or pandemics further aggravate the process of diagnosis and treatment process. The inefficiency of approaches warrants for the development of a robust diagnostic method that can be used in regional medical clinics that lacks the capabilities for performing conventional diagnostic assays. Current approaches involve use of nanomaterials (NMs) in diagnosis with special emphasis to utilizing NMs' unique physico-chemical properties for biosensing of molecular recognition with greater speed, sensitivity and specificity. Integrating microfluidics platform with NMs-mediated biosensing

View Article Online
DOI: 10.1039/D0AN00896F

regimes has the potential to address future PoC devices, which can be used in remote settings without having to rely on centralized clinical laboratories (Fig. 2).[29, 30]

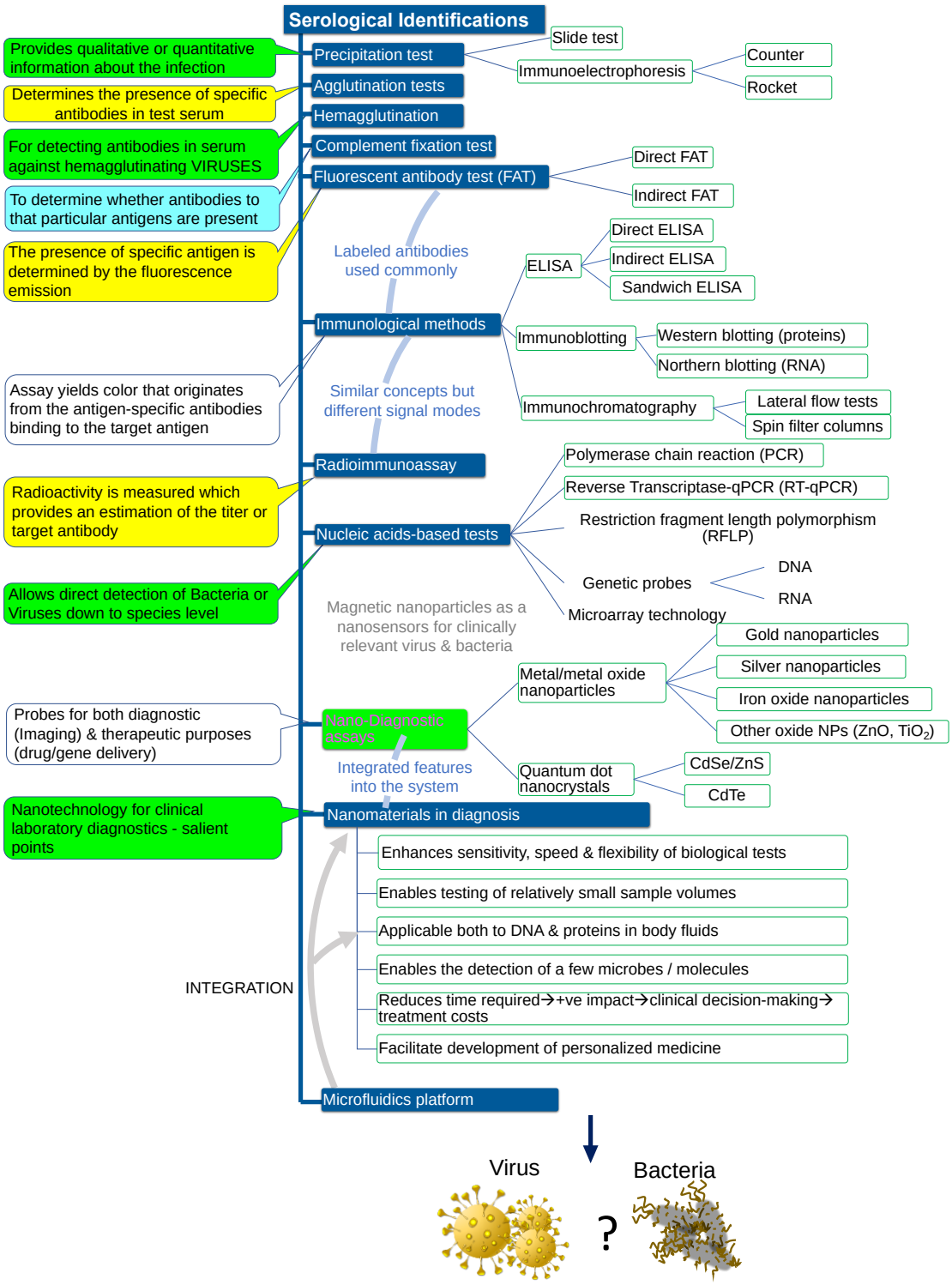

View Article Online
DOI: 10.1039/D0AN00896F

Fig. 2. Serological methods used conventionally for the diagnosis of bacterial or viral infections and current trends involving integration of microfluidics, nanomaterials for point-of-care for disease diagnosis.

3. Biomarkers for detection of viral and/or bacterial infections

One of the most common medical problems community has been facing is the differentiation of viral infection from bacterial infections or vice-versa due to their identical symptoms. Yet, there is likely 50% chances that the viral infections may be misdiagnosed for bacterial infections and therefore, prescription of antibiotics is followed to avoid further risks of propagation of life-threating pathogenic bacteria. Diagnosis of bacterial/viral infections is one of the areas that require more research for early diagnosis and prognosis, such as by screening for host biomarkers as signatures in bodily fluids. The ideal host infection biomarker should be able to differentiate between an infected patient and a normal individual without infection, along with its etiology of infection (bacterial or viral).[31] An ideal bacterial/viral infection host biomarker should have the following characteristics, such as; (a) a positive test result in infected patient, (b) a negative test result in patients without an infection, (c) differentiate etiology, (d) independent of comorbidities, (e) a predictor of severity, (f) a predictor of outcome, (g) a quick and easy test with minimum error and (h) affordable. Further, an ideal biomarker require to be independent of the duration of febrile illness and of comorbidities, as well as easily and quickly measurable characteristics from minimally invasive samples.[31] As per the standpoint of diagnostics and prognostics, the infection biomarkers can be classified into therapeutic and pathogenetic biomarkers that play a critical role with clinical significance.

Most of the studies are related to testing one or more host biomarkers which were generated by the bodily immune responses to infections (Fig. 3a-c). The host immune response responds to infection by releasing molecules into the circulatory system that reflects real-time pathological changes taking place in the body. Concentrations of these molecules released into the bloodstream has biological significance because of their involvement in various pathological processes and therefore serve as target biomarkers. However, not all of these molecules are suited to this aim but should fulfill certain conditions.[32] The primary host biomarkers include host proteins, gene transcripts, cellular processes/biochemical reactions.[32] Recently, the most frequently studied host biomarkers are summarized in relation to their different mechanisms involved in the development and autoimmune responses of the human body against any host bacterial/viral infections (Fig. 3a-b).[32, 33] Kapasi et al. (2016) reported statistical significance of classified eight-sets of host candidate biomarkers that are potentially high performance bodily fluid

View Article Online
DOI: 10.1039/D0AN00896F

markers (these include plasma, saliva and cerebrospinal fluid (CSF)) for bacterial and viral infections (Fig. 3b-c).[32]

View Article Online
DOI: 10.1039/D0AN00896F

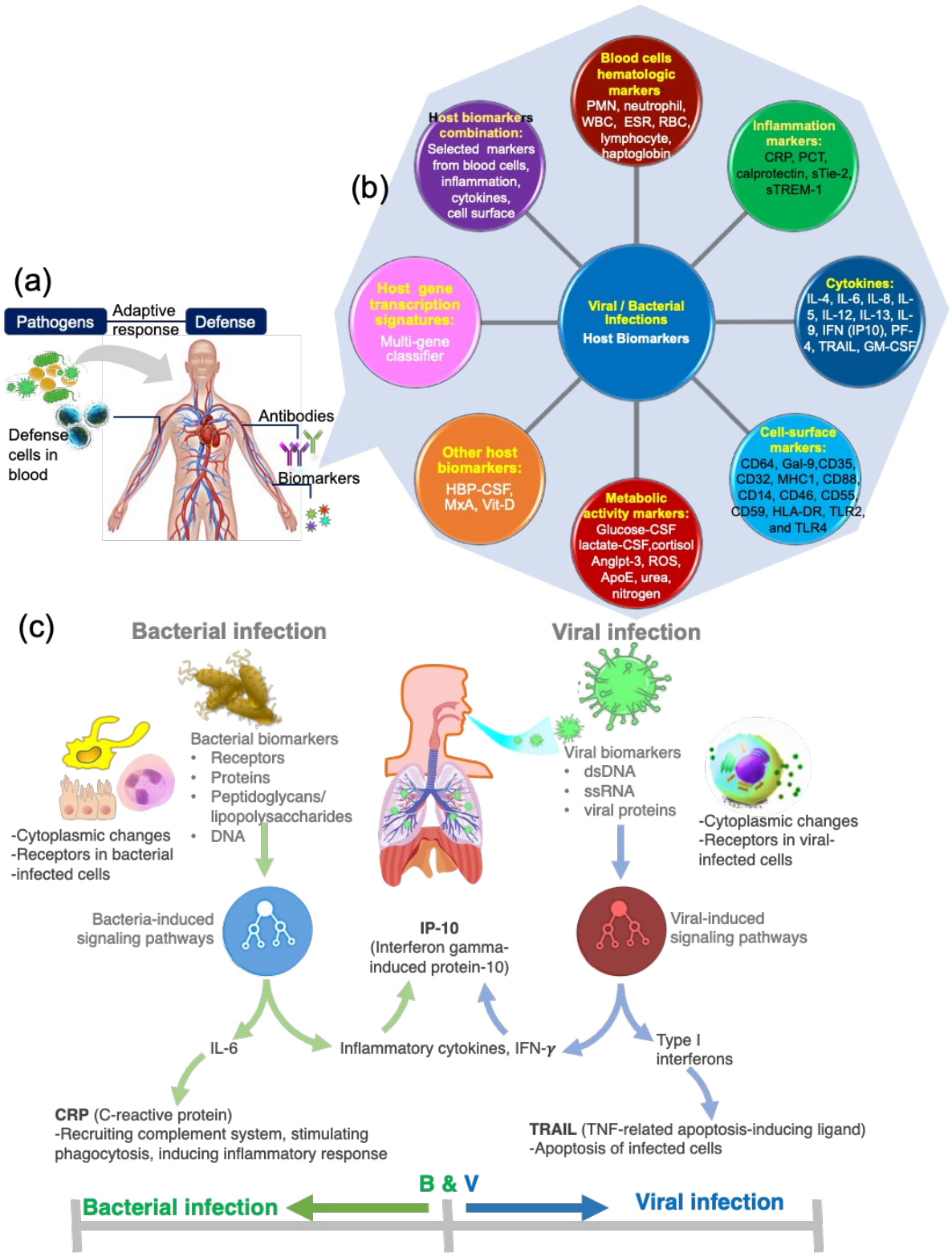

Fig. 3 (a) Schematic illustration of elevated target biomarker levels generated because of adaptive response against viral and bacterial infections, (b) most frequently studied bacteria/non-bacterial infection

View Article Online
DOI: 10.1039/D0AN00896F

biomarkers in relation to the different mechanisms involved in respiratory infections [31-34] and (c) Recent approaches to differential diagnosis of viral and bacterial infections is carried out using circulatory proteins, such as C-reactive protein (CRP) and interleukin-6 (IL6) for bacterial infections and TNF-related apoptosis-inducing ligand (TRAIL) and interferon gamma-induced protein-10 (IP-10) for viral infections.[35-38] Different protein levels tend to increase during bacterial (B) or viral (V) infections, respectively are shown at the bottom.

High-performing hematologic host biomarkers with statistically significant findings include polymorphonuclear leukocyte (PMN), neutrophil counts, white blood cells (WBC), erythrocyte sedimentation rate (ESR)[31, 32, 39] and Human Neutrophil Lipocalin (HNL) counts.[40] The levels of PMNs or phagocytes are often reported to be elevated in blood and considered to play a major role in the defense response of the host during an infection episode.[41] These cells inherit different sets of information in cases of different etiological agents stimulating immunity and therefore, act as disease biomarkers in a specific infection environments.[12] WBCs originate from the bone marrow and circulate throughout the bloodstream, also referred to as leukocytes. The immune system is mainly characterized through WBCs due to its physiological function to fight against infections from bacteria, viruses or fungus that invade the body. The normal range of WBCs is reported to be in the range 4500–11500 μL^{-1} in healthy conditions. It has been reported that WBC concentration above 11500 μL^{-1} is related to leukocytosis condition[42, 43] and linked with bacterial infection rather than viral infection and serves as a strong biomarker candidate to differentiate bacteria over viral infection.[32, 44] WBC concentration <4500 μL^{-1} is related to leukopenia condition and linked to long-term use antibiotics and also chemotherapy in cancer.[42] Therefore, WBC concentration is considered to have high diagnostic significance in acute infection and chronic disease management. The ESR level test is another important disease biomarker because erythrocytes have a tendency towards rouleaux formation since large aggregates of cells settle more quickly than individual erythrocytes.[45, 46] In infectious disease condition, the increasing rouleaux formation reduces the zeta-potential of erythrocytes due to increase in plasma fibrinogen, immunoglobulins and other acute-phase-reaction proteins, which enables ESR as indicative signature of diseases condition.[45]

Inflammation markers, such as C-reactive protein (CRP), procalcitonin (PCT) showed statistically significant differences in bacterial versus non-bacterial infections.[31, 32, 35, 47-50] CRP in humans is a Ca-dependent ligand-binding plasma protein which is composed of a cyclic homo-pentameric non-glycosylated polypeptide sub-units.[51] It is an acute phase protein which primarily synthesized in response to factors related by macrophages in liver. CRP is identified as both infection and inflammation biomarker in clinical diagnosis settings. Bacterial elimination by macrophages were linked with CRP

View Article Online
DOI: 10.1039/D0AN00896F

binding with phospholipid constituents of bacteria.[51, 52] The kinetics of CRP responses proved it as a sensitive and specific biomarker to improve the differential diagnosis between acute bacterial (68–92%) and viral infections (40–67%). [53] It has many functions that mainly include activation of classical complement pathway and modulation of immune cells' functions and cellular cytotoxicity.[54] CRP was examined as a protein in patients with pneumococcal pneumonia during pneumococcal C-polysaccharide precipitation process[31] and served as a strong candidate for severity of infection and enable early diseases prognosis and treatment progression.[53] Whereas, PCT is a precursor of hormone calcitonin, secreted by the C cells of the thyroid gland in human.[55] It is a pro-peptide of calcitonin and composed of 116 amino acids and has a molecular weight of 13 KDa.[56] PCT levels are a critical parameter for inflammation and is now well recognized for acute and severe bacterial as well as viral infections. As it is known that pneumonia is the key LRTIs during which the level of PCT found to be high on first day of LRTIs. It is reported that both CRP and PCT could serve as predictive diagnostic indicators when combined with other biomarkers.[31, 32, 35, 40, 47-50] Infection screening in hospitals is commonly performed by; (a) blood tests (such as WBC count, C-reactive protein (CRP) levels and blood culture) for screening large number of clinical samples combined with (b) chest X-ray for abnormalities in lungs, heart and blood vessels and, (c) lumbar puncture for WBC count in spinal fluid.

Other class of host protein biomarkers are cytokines and these are the mediators of inflammatory response against invading pathogens and serve as infection biomarkers. Cytokine species can be categorized into two groups namely, pro-inflammatory cytokines, such as mainly IL-1, IL-2, IL-6 and IL-8 and TNFα and anti-inflammatory cytokines, such as IL-4, IL-10 and IL-13 [57]. The most significant performance in cytokine infection biomarker family were Interferon (IFN) gamma-inducible protein 10 (IP-10; also known as CXC motif chemokine 10, CXC10), TNF-related apoptosis-inducing ligand (TRAIL), interlukin-2 (IL-2), IL-4, IL-6 IL-8 and IL-10.[32] Pro-inflammatory chemokine, IP-10 is secreted by cells (neutrophils, monocytes, macrophages and endothelial cells) responsible for trafficking Th1 lymphocytes to inflammatory-foci.[58] IP-10 shown to be highly sensitive and specific biomarker candidate for the immune-diagnosis of TB infection based on the measurement of IP-10, following stimulation with *Mycobacterium tuberculosis*-specific antigens[59] (Fig. 3a-c). Furthermore, IP-10 considered to be as a surrogate to identifying and validating the treatment response in patients with TB infection.[59] TRAIL biomarker is the member of the tumor necrosis factor (TNF) family and studies have shown that it plays an important role in programmed cell death.[35] TRAIL was found to be induced to a wide range of viral infections in patients with suspected acute infectious disease (Fig. 3a-c). Also, it showed reduced levels in bacterial infected patients. TRAIL particularly suitable for distinguishing between bacterial and viral infections due to its dynamic level change in bacterial and viral infections[35] (Fig. 3c). The increased levels of TRAIL in viral patients has been previously linked to programed cell death and this event is one of the

View Article Online
DOI: 10.1039/D0AN00896F

possible mechanisms by which infected cells attempt to inhibit the virus from spreading.[35] IL-6 is an important biomarker and compose of glycoprotein (21 kDa) produced mostly by macrophages and lymphocytes. It plays a major role in activation and accumulation of lymphocyte and macrophage accompanied with secretion of Monocyte Chemoattractant Protein-1 (MCP-1).[60] The levels of IL-6 were reported to be high in patient with severe infection and therefore served an indicator of disease severity [61]. Among the above cytokines, IP-10 and TRAIL combined with other biomarkers showed high and promising diagnostic values.[32]

With respect to other markers, 13 of the cell surface markers were identified to differentiate bacterial and non-bacterial infections. These include several cluster of differentiation (CD) proteins, mainly CD64, CD35, CD32, galectin (Gal)-9, MHC1 (major histocompatibility complex class 1), CD14, CD46, CD55, CD59, CD88, human leukocyte antigen (HLA)-DR, toll-like receptors (TLR2 and TLR4). However, combination of CD35, +CD32,+CD88,+MHC1 cells surface biomarkers exhibited significant higher performance to bacterial and viral infections.[32] The most frequently examined metabolic activity markers were found to be the above indicated 13 cytokines and that should also include total protein and glucose concentration in cerebrospinal fluid (CSF). Among them, lactate-CSF showed high diagnostic performance for discriminating bacterial and non-bacterial infections. Recently, other host biomarkers, such as Homeostasis marker-heparin-binding protein (HBP)-CSF, antimicrobial biomarker response-myxovirus resistance protein 1 (MxA),[32] and serum vitamin D levels[34] found to be effective and reliable biomarker that discriminate bacterial and non-bacterial infections. The link between the susceptibility to infection and the low levels of vitamin D found to be associated with respiratory system infection and therefore, vitamin D levels can serve as an RTI biomarker.[62] Host transcription signatures also shown to be promising biomarkers, these were identified on multi-gene classifier transcriptional profiling.[32] The combination of PCT and 10-Gene classifier exhibited promising diagnostic results to differentiate bacterial from viral LRTIs. Another study also showed that 48-gene classifier could be used to detect H3N2 influenza and can discriminate between viral respiratory and bacterial infections.[32, 63]

It is difficult to select a specific marker for the differential diagnosis of bacterial/viral infections. Therefore, a range of biomarkers and their combinations have emerged as strong and reliable risk predictors, which can potentially be analyzed simultaneously for the accurate differentiation in bacterial and viral disease diagnosis, as listed in Table 2.[31, 34, 39, 40, 44, 50, 64, 65] Of which, CRP has been the most frequently used in combination with other biomarkers such as IP-10 and TRAIL for discriminating between viral and bacterial infections. According to recent reports, a cut-off value for a moderately elevated CRP levels for viral RTIs was 10-60 mg/L[31, 32, 35, 50, 66, 67] and >100 mg/L[31, 32, 35, 47-50] for bacterial infection, with a peak during 2–4 days of illness. It is reported that moderate increase in CRP levels during the illness of less than 7-days cannot determine bacterial infection. However, it may indicate a

View Article Online
DOI: 10.1039/D0AN00896F

complication due to a viral infection after a week of illness. Another two important host biomarkers such as TRAIL and IP-10 biomarkers were promising in distinguishing viral infections. The level of TRAIL >2.2 μg/mL was related to viral infection[68] and for bacterial infection, its level found to be much lower with <50 pg/mL, indicating its specificity to viral infections[35]. In case of IP -10 for viral infection, the cut-off level is reported to be >150 pg/mL,[69, 70] whereas for bacterial infection its level could go up to 600 pg/mL[35] and in case of co-infection (Bacterial + Viral), the IP-10 level shifts to much higher level to <1.5 ng/mL.[35, 71] The three biomarkers namely, CRP, TRAIL and IP-10 were found to be promising biomarkers for differentiating bacterial and viral infections. Further, multi-biomarkers detection from the same sample, such as by combination of a panel of CRP, TRAIL and IP-10 can be more effective diagnostic approach to accurately differentiating bacterial and viral infections compared to relying on detecting a single or random biomarker (Fig. 3c).[72] In a recent report, different biosensor platforms have been reviewed that specifically targeted detection of similar cytokine/protein biomarkers in sputum and saliva for diagnosis of chronic obstructive pulmonary disease (COPD)[73] and presented mechanisms and biomarkers of COPD pathophysiology that also common to RTIs (Fig. 4). However, low levels of sputum/salivary biomarkers present challenges in detection and differentiating bacterial and viral infections.

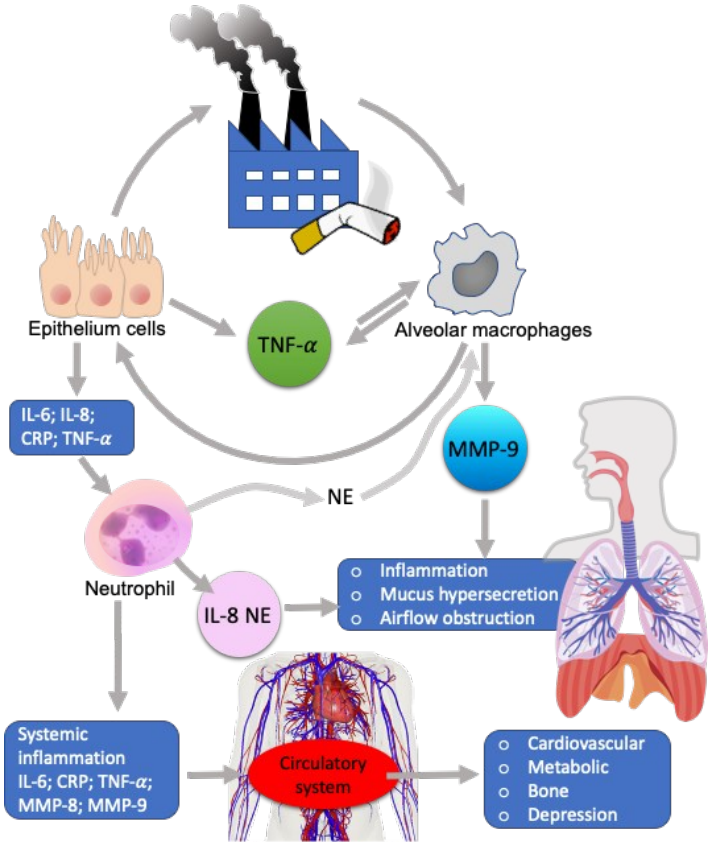

View Article Online
DOI: 10.1039/D0AN00896F

Fig. 4. Schematic representation of the inflammation responses and biomarkers of coronary obstructive pulmonary disease (COPD) pathophysiology caused by environmental stimulus that can also be common/linked to respiratory tract infections (RTIs).[73] Interleukins (ILs 6 and 8), tumor necrosis factor-alpha (TNF-α), Neutrophil elastase (NE), C-reactive protein (CRP), matrix metalloproteinase (MMP-8 and 9) and serve as biomarkers with promising clinical value that can be applied for detecting host responses to infections from viral and/or bacterial origins.

Immediately after the bacterial/viral infections, the body releases multiple biomarkers into the bloodstream toward circumventing the progressive infection. An ideal biosensor should be able to pick these signals through sensing the released biomarkers in a relatively short time, which could help improve clinicians in rapid, real-time and accurate diagnosis. Elevated concentrations of these predictive multiple infection markers in biological fluids, such as from serum, urine or CSF can infer the process of infection. To accurately design a patient care strategy, simultaneous determination of biomarker levels is essential for clinicians to quickly diagnose bacterial/viral infections. Rapid and reliable detection of infection biomarkers helps medical professionals to make accurate clinical decisions as well as differentiate diseases from other similar symptoms. Clinically significant detection ranges of potential biomarkers of infections (such as CRP, TRAIL, IP-10) are extremely low (pg/mL to ng/mL) and assay methods for detecting such biomarkers requires high sensitivity. In this context, various biosensor platforms have been designed for detection of potential bacterial/infection. In this review, we summarized the most prominently used bacterial/viral biomarkers and their detection by different biosensor platforms. Few of biomarkers such as CRP, PCT and cytokine biomarker family are considered to be useful for differential diagnosis of infectious diseases (bacteria/viral/sepsis) as well as for inflammatory diseases (cardiovascular risk/ chronic diseases). A number of reviews have already been reported on biosensors for diagnosis and detection of sepsis and cardiovascular disease.[16, 60, 74] Therefore, current review excludes the biosensing platforms which are mainly reporting to detect selected common biomarkers for inflammation and/or sepsis.

4. Biosensors for bacterial/viral infection biomarkers detection

A biosensor is a device designed to detect and quantify target molecules (e.g., proteins, nucleic acids or monitoring antigen–antibody interactions) used widely as a powerful analytical tool in medical diagnostics. It is generally designed by immobilizing a biological receptor ligand (e.g., antibody, receptor, DNA, or RNA) on the surface of a suitable transducer (e.g., electric, electrochemical, optical or mechanical) that converts biochemical signal into quantifiable measurable signal. In the past few years, a large number of sensors have been developed for bacterial and viral infection biomarkers detection, which

View Article Online
DOI: 10.1039/D0AN00896F

can play a major role in differentiating bacterial and viral infection. A summary of distinct biosensor platforms available for the detection of bacterial/viral infections in the research laboratories is presented in Tables 1 and 2 along with the most prominently used viral and bacterial biomarkers. These biosensor platforms provided fruitful outcomes through integrating nanomaterials in combination with interdisciplinary research-works, which further contributed to the advancement in biosensors for diagnosis of infectious diseases.

Table 1. A summary of primary clinically high performance predictive host infection biomarkers based on statistically significant findings, highlighting their respective cut-off values.

Host biomarker for primary care setting	Sample	Healthy levels [#]	Bacterial infection [#]	Viral infection [#]
Polymorphonuclear leukocyte (PMN) counts	CSF/blood	119±311 cells/μL in blood[75]	Cut-off:30–49 cells/μL in CSF; 18±19 in blood[32, 75]	NA
Absolute neutrophil count (ANC)	Blood	Cut off: 4900 to 10000 cells/μL[32]	<1500 cells/μL[76]	NA
White blood cell count (WBC)	Blood	4500–11500 cells/μL[42, 43]	Cut-off:7200 to 17000 cells/μL[31, 32, 39]	25-500 cells/μL in CSF[77]
Erythrocyte sedimentation rate (ESR)	Blood	≤19 mm/h in males; ≤23mm in females[78]	Cut-off:≥ 25.5 to ≥32.5 mm/hr.[32, 79]	NA
Monomeric (m) and dimeric (d) Human Neutrophil Lipocalin (HNL) counts	Serum	m-23 (IQ,15–35) μg/L; d-76 (IQ, 60–96) μg/L[14, 40]	m-169 (IQ, 93–306) μg/L; d-304 (IQ, 205–457) μg/L[14, 40]	m-48 (31–84) μg/L; d- 78 (64–106) μg/L[14, 40]
C-reactive protein (CRP)	Blood	<10 mg/L[31, 32, 80]	>100 mg/L[31, 32, 35, 47-50]	10-60 mg/L[31, 32, 35, 50, 66, 67]
Procalcitonin (PCT)	Blood	0.033±0.003 ng/mL[81]	≥2.0 ng/mL[31, 32, 50]	NA
Interferon gamma-induced protein-10 (IP-10 or CXCL10)	Blood	<150 pg/mL[32, 69, 82, 83]	• 600 pg/mL [35] • Co-infection (Bacterial + Viral) <1.5 ng/mL[38, 41, 75, 86]	>150 pg/mL[32, 69, 82, 83]
Tumor necrosis factor (TNF)-related apoptosis-inducing ligand (TRAIL)	Blood	<822 pg/mL[50, 68, 83]	<50 pg/mL[35, 50, 83]	>2.2 μg/mL[50, 68, 83]
Interleukin-4 (IL-4)	Blood	Cut off: 9 pg/mL[32]	1.47 pg/mL[84]	0.99 pg/mL[84]

Lactate	CSF	3.8 mmol/L[32]	≥6 mmol/L[85]	3~6 mmol/L[85]
Heparin-binding protein (HBP)	CSF/Serum	Cutoff 56.7 ng/mL in CSF; 45.3 ng/mL in serum	192 ng/mL in serum[86]	3.7 ng/mL in serum[86]
Myxovirus resistance protein 1 (MxA)	Blood	36.7 ng/mL[32]	NA	200 ng/mL[87]
Vitamin D	Blood	19.5 ng/mL[88]	10.7 ng/mL[88]	<20 ng/mL[34]
PCT +10-Gene classifier	Blood	-	Respiratory infection[32]	Respiratory infection[32]
48-Gene classifier	Blood	-	Respiratory infection[32]	Respiratory infection[32]
Combination of host biomarkers				
CRP,+IP-10,+TRAIL	Blood	CRP (<10 mg/L); TRAIL (<822 pg/mL); IP-10 (<150 pg/mL)	Cut-off: CRP ~135 µg/mL, IP-10 ~600 pg/mL, TRAIL ~50 pg/mL[32]	Cut-off: CRP ~125 µg/mL, IP-10 ~800 pg/mL, TRAIL ~150 pg/mL[32]
HNL, IP-10 and/or TRAIL	Blood	HNL (m-23 (15–35) µg/L; d-76 (60–96) µg/L); IP-10 (<150 pg/mL); TRAIL (<822 pg/mL);	High HNL profile[40]	High IP-10 and TRAIL profiles[40]
CD35, +CD32,+CD88,+MHC1	Blood	-	Cut-off: CD35 B 151×10^3 cells/neutrophil, CD32 158×10 cells/monocyte; CD88 ~112×10^3 cells/monocyte; MHC1 ~ 0.40 ratio[32]	Cut-off: CD35~45×10^3 cells/neutrophil; CD32~65×10^3 cells/monocyte, CD88~ 47×10^3 cells/monocyte, MHC1~ 0.28 ratio[32]

NA – not available; IQ- Interquartile range; #- concentrations of proteins/antibodies are subject to vary in the literature, the listed concentrations are selected based on either supported by two independent studies or from available ELISA ranges

Table 2. List of bacterial/viral infection-induced host biomarkers sensing with different sensor platforms and their range of detection as per the reported literature.

Biomarker / Target	Transducing platforms	Ranges of detection	Assay-type	Reference
PMN counts	Fluorescence-PBS	ND, proof of concept	Microfluidic with smart phone, single analyte	[89]
PMN counts	Chemiluminescent (CL)	ND, proof of concept	Luminol-dependent CL- phagocytes	[12]
PMN,PBMC, WBC, RBC	FL-staining	A single step centrifugation of the CMC for 10 min could achieve both recovery and purity rates >95% for PBMCs, a WBC viability rate >98%,	Centrifugal microfluidics chip, multianalyte	[90]
Neutrophil elastase	FRET- fluorogenic	K_M ~0.7 μM, PBS buffer pH 6.2, 25 °C	Protein-based fluorescent substrate on 96-well plates-transducing surface, single analyte	[91]
WBC, HIV	Magneto-immunoassays	HIV in saliva with an accuracy of 80% and leukocytosis in plasma with an accuracy of 90%	Changes in Giant Magnetoresistance chip biosensor with smartphone interface, multianalyte	[92]
WBC/RBC	Impedance cytometer	WBC/RBC counts-1000 cells/s	Polyelectrolyte salt bridge-based electrode integrated with microfluidic chip	[93]
WBC	Electrochemical	WBC dynamic range -10^2–10^4 μL^{-1}	Microelectrode based electrochemical cell with smartphone interface	[43]
ESR	Conductivity sensor	Proof of concept- ESR depends on blood conductivity within 400 seconds	Two planar electrodes	[94]
CRP	Electro-chemiluminescence	1–24 μg/mL	Anti-CRP-Ru-(bpy)32+ modified Au working electrode, single analyte	[95]

CRP	Giant magnetoimpedance	Linear range 1-10 ng/mL	Micro-patterned GMI sensing elements-cobalt-based commercial amorphous ribbon (Metglas® 2714A)	96
CRP, Mycobacterium tuberculosis lipoarabinomannan (LAM)	Optical sensor-spectral analyzer consisting of an arrayed-waveguide grating	LOD was 19.478 ng/ mL	Lab-on-a-chip SiN anti-reflective coated photonic sensor	97
CRP	QCM	LOD- direct assay and the homogenous sandwich assay: 20 ng/mL whereas for the direct sandwich assay: 3 ng/mL	Immunoassay based on Resonant Acoustic Profiling™ (RAP™), single analyte	98
CRP	Electrochemical	LOD: 37 nM	Conducting polymer electrode, single analyte	99
CRP, PCT	Electrochemical/Non-Faradaic	LOD - 0.1 µg/mL for CRP; 0.1 ng/mL for PCT	ZnO film-based electrode	100
CRP, biotinylated bovine serum albumin (BSA)	Plasmonic biosensor	27 pg/mL of CRP and 10 pg/mL of bBSA	Gold nanohole based plasmonic micro arrays	101
CRP, IL6 and miRNA-16	Optical-interferometric biosensor	LOD:18 µg /mL for CRP, 88 µg/ mL for IL6 and 6 µg /mL for miRNA-16	Optical path difference on plasmonic gold nanohole array chips, multianalyte	102
PCT, CRP	Electrochemical	LOD: PCT 0.09 ng/mL and CRP 0.008 µg/mL	Magnetic bead-based immunoassay on screen-printed electrodes	103
PCT	Electrochemical	Binding constant of 0.39 ± 0.11 nM	Synthetic peptides-based EC gold sensor	104
CRP, IL-6	Electrochemical	LOD- 1 pg/mL for both CRP and IL-6	Molybdenum electrodes on nanoporous polyamide substrate	105
IL-6	Optical-colorimetric	LOD-0.1 pg/mL	plasmonic gold nanoprobes t	106

CRP	Optical-imaging	0.2 ~ 20 ng / mL, LOD: 0.1 ng/mL	Magnetic-particle probes on microfluidic chip for total internal reflection magnetic imaging	107
CRP	Electrochemical/potentiometric	1.0×10^{-5} mg/L to 1.0×10^{0} mg/L	ZnO nanotubes-based electrode	108
CRP	Electrochemical/ impedimetric	0.5–50 nM	Au-electrode	109
CRP	Optical-FL	800 aM to 500 fM	Imaging-molecular switching of fluorescence by total internal reflection	110
CRP	Optical-	2 to 20 mg/L	Polymer/aptamer films for optical fiber refractometers based on Lossy Mode Resonances (LMRs).	111
CRP	Optical-refractive index	0.1–10 μg/mL	MCLW sensor chip with nitrocellulose based on surface sensitive refractive index	112
CRP	Optical-FL	27.8 pM	Fluorescent CdSe/ZnS quantum dots (QDs) nanospheres (IFNs)	113
CRP	Optical-SPR	2–5 μg/mL	Gold chip based SPR	114
CRP	Optical-SPR	~50 ng/mL	Gold nanoparticles grafted with polymerized specific ligands based SPR	115
IL-6, IL-8, IL-10, TNF alpha, S-100, PCT, E-Selectin, CRP and Neopterin	Optical-FL scanning	1.2 pg/mL, 0.89 ng/mL, 2.7 ng/mL, and 0.13 μg/mL for IL-6, IL-8, IL-10, TNF alpha, S-100, PCT, E-Selectin, CRP and Neopterin, respectively	Fluorescence microarray scanning assay-based streptavidin coated magnetic particles	116
CRP, PCT, Lactate	Hybrid-biochemical-immunological	CRP: 0.01 μg/mL and 100 μg/mL, PCT: 0.01 ng/mL and 10 ng/mL, lactate: 9 mg/dL to 72 mg/dL.	Enzyme-reaction zone on the signal pad of the typical immuno-strip based on 2D-chromatography	117
CRP	Electrical-FET	LOD: 0.1 ng/mL	Nano-gap embedded FET electrode	118

CRP	Electrochemical-amperometric magnetoimmunosensor	LOD: (0.021 ± 0.005) ng/mL	sandwiched immunoassay assay based on magnetic bead- Au/SPE	119
CRP	Colorimetric	Linear range 0.03–81 ng/mL and a LOD of 0.07 ng/m	GNPs covalent attachment of antibody-sandwich assay	120
PCT	Optical-TIRF	0.04 ng/mL	Fluorescence labeled tracer on transparent core	121
PCT	Optical-SPR	9.9 ng/mL	Molecular imprinted polymer surface on SPR slide	122
PCT	Optical-SPR	4.2 ng/mL	Gold coated SPR chip	123
PCT	Electrochemical	0.03 pg/mL	Cu/Mn double-doped CeO_2 nanocomposite (CuMn-CeO_2) signal tag on gold deposited GCE	124
PCT	Electrochemical/amperometric	0.8 pg/mL	Ferrocene-modified gold nanoparticles-based electrode	125
PCT	Electrochemical	6 pg/mL	PtNP-Fc-C_{60} nanocomposites.	126
PCT	Electrochemiluminescence	3.4 pg/mL	CdTe quantum dot encapsulated silica nanoparticle tags with nanobodies	127
PCT, LTA, and LPS	Electrochemical	LOD: PCT-0.1 ng/mL, 1 µg/mL for LPS and LTA	Nanoporous nylon membrane integrated onto a microelectrode sensor	128
PCT	Electrochemical	0.1 pg/mL	Gold nanoparticles-enhanced tyramide signal amplification	129
PCT	Optical	7.3 fM	Fiber optic nanogold-linked immunosorbent assay	130
IL-2, IL-4, IL-6, IL-10, TNF-α, and IFN-γ	Optical-LSPR	IL-2: 20.56 pg/mL, IL-4: 4.60 pg/mL, IL-6:11.29 pg/mL, IL-10:10.97 pg/mL, TNF-α:11.43 pg/mL, IFN-γ: 6.46 pg/mL	Gold nanorods nanoplasmonic microfluidic chip, multianalyte detection	131

View Article Online
DOI: 10.1039/D0AN00896F

4.1. Optical biosensors

A range of bacterial and viral biomarkers have been detected on different optical biosensor platforms that are based on fluorescence, chemi-luminescence, colorimetric, surface plasma resonance (SPR) and fiber optics/bio-optrode transducers. Current studies are focused on improving methodologies for both single and multi-analyte detection schemes, as well as integration of immunosensors with smart phone and microfluidic biochip platforms.

Several optical biosensor platforms have been developed for the detecting bacterial and viral biomarkers, where immunosensors were integrated into microfluidic platforms, such as for capturing leukocytes from biological sample.[89] The designed biosensor chip is fabricated using polydimethylsiloxane (PDMS) on glass slide that carried dense microfluidic channels and demonstrated proof of concept for capturing leukocytes from biological sample by antigen antibody interaction. The signal from the biochip is captured by fluorescence imaging using a smartphone and quantified using image processing software, and this method is suitable for biosensing infections in resource limited settings (Fig.5-b).

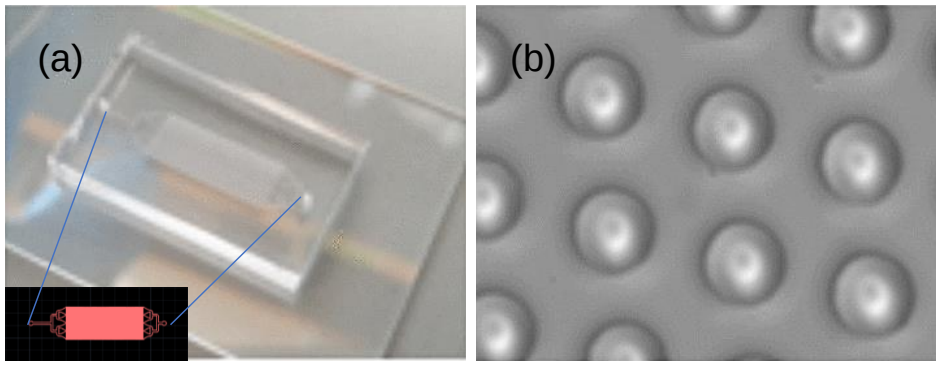

Fig. 5. (a) Designed microfluidic biochip to process the biological samples and capture the leukocytes. The inset diagram shows schematic design pattern showing dense microfluidics channels through which leukocytes were captured and (b) microscopic image of the capture chamber pillars in biochip.[89]

In another study, a chemiluminescence based assay was developed to characterize polymorphonuclear leukocytes (PMNs) or phagocytes functional activity and assessed reaction byproduct by quantification and localization of respiratory burst production by chemiluminescent (CL) measurements.[12] This assay was tested for the PMNs of patients with acute infections from whole blood system that required luminol-

View Article Online
DOI: 10.1039/D0AN00896F

amplification for CL measurements. CL is considered a sensitive sensing method for probing oxidative potential of phagocytes, which can be recorded as a luminol-dependent CL. The reported method used blood sample from 69 patients with fever (>38 °C) and diagnosed infections caused by viral or bacterial in origin. The CL measurements combined with different data mining algorithms allowed to discover specific patterns for each type of infection. Analysis of a relatively large number of patients samples generated a pool of CL-data, which upon processing with the help of an algorithm (data mining), generated interpretable model as a decision tree for accurate and rapid differential diagnosis (Fig. 6).[12] Such approaches could also be applied to various other sensing schemes to generate a highly predictive diagnostic value that potentially assist clinicians in diagnosis, as well as distinction between viral and bacterial infections.

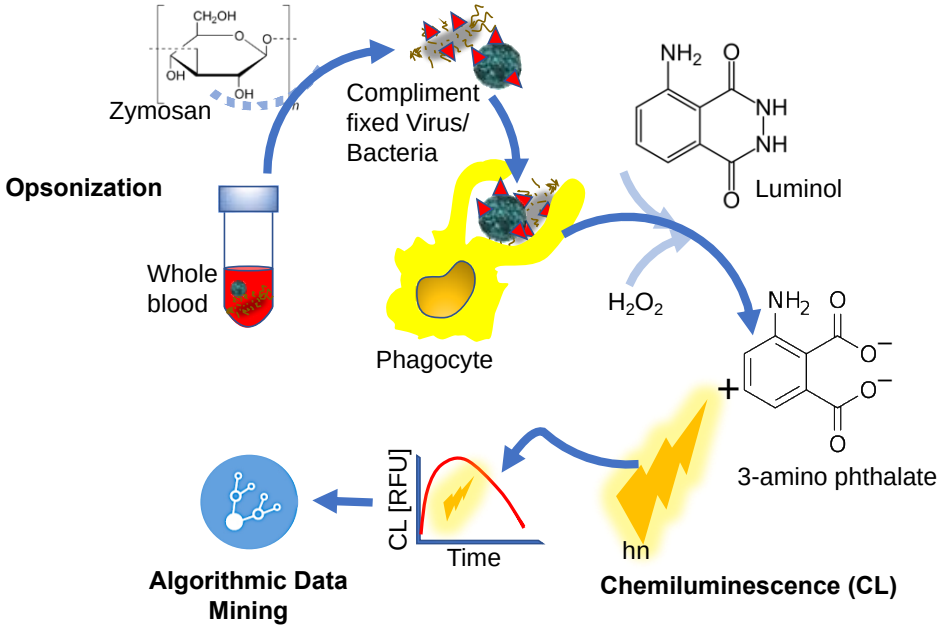

Fig. 6. Schematic diagram of chemiluminescence (CL) assay for circulating PMNs or phagocytes from whole blood sample and differentiation between viral and bacterial acute infections. The assay allows quantification and localization of respiratory burst production from circulating PMNs or phagocytes and the byproduct of chemiluminescent (CL) reaction is measured. The CL-data thus generated is then subjected data mining for interpretation that generates decision tree and confusion matrix of patients in the training and testing sets to accurately detect and differentiate viral and bacterial infections.[12]

Further, Yu et al. reported a centrifugal microfluidic chip (CMC) for sorting immune cells, such as polymorphonuclear cells (PMN-Neutrophils, eosinophils and basophils), and peripheral blood

View Article Online
DOI: 10.1039/D0AN00896F

mononuclear cells (PBMCs- lymphocytes and monocytes), WBC and RBC from blood.[90] The chip operation for sorting cells from a blood specimen is carried out by density gradient centrifugation within the microfluidic channels, which effectively sorted immune cell subpopulations into distinct layers that depended on their specific densities. This report utilized conventional blood centrifugation process but by using a density gradient medium (DGM), such as the Ficoll or Percoll solution to fractionate and sort blood cells into different layers using their inherent distinctive densities (Fig. 7-I:a).[132] During density gradient centrifugation, different blood cells in a bulk fluid migrate to different density equilibrium positions (Fig. 7-I:b). This technique was integrated in a miniaturized microfluidic centrifugation systems and demonstrated multi-color fluorescence imaging while restoring the capability of separated whole blood into multiple cell layers (Fig. 7 -II). This method demonstrated a single step centrifugation of the CMC within 10 min with recovery and purity rates of >95% for PBMCs, >98% for WBC viability rate, and stable separation within the channel from minimally processed whole blood.

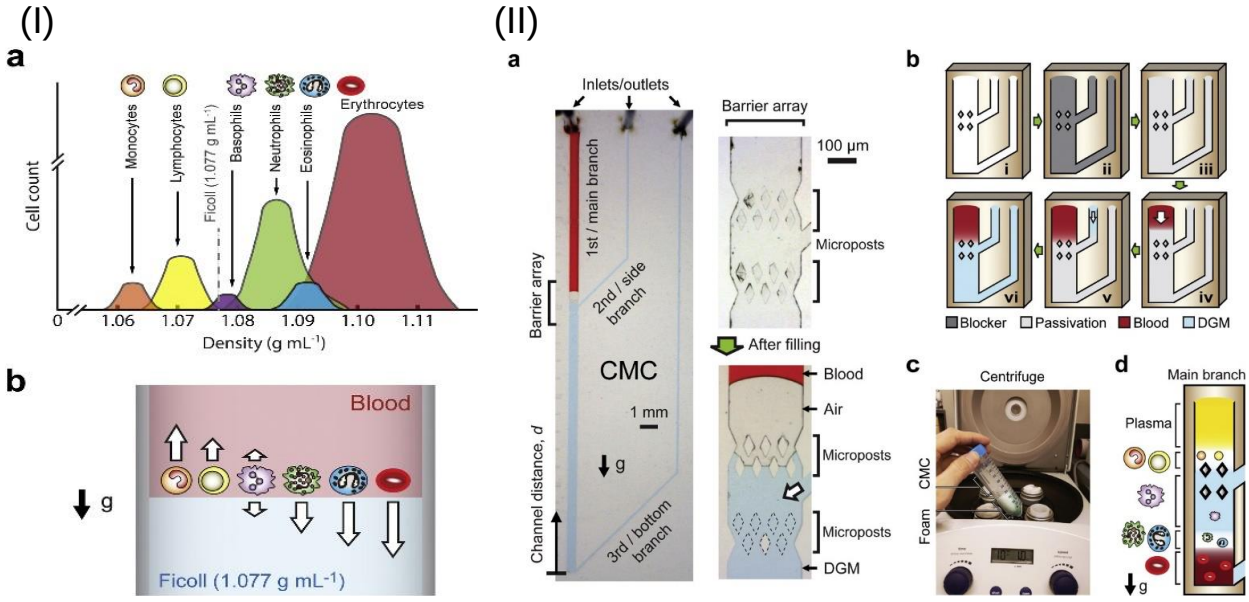

Fig. 7. I:(a-b). Blood cell densities and sorting using density gradient centrifugation.[90, 132] II:(a-d) Blood cell sorting using density gradient centrifugation in a microfluidic device.[90]

A neutrophil elastase (NE) specific-protein sensor has been reported that utilizes förster resonance energy transfer (FRET) for detection of infection. The biosensor assay involves two fluorescent green fluorescent protein (GFP)-derived proteins linked by a peptide linker containing a NE-specific recognition sequence bringing both to a close proximity to exhibit FRET. The decrease in FRET signal occur upon selective cleavage of GFPs by NE which was measured and demonstrated the sensor capability to

View Article Online
DOI: 10.1039/D0AN00896F

recognize sequence as well as detecting NE.[91] In another study, an anodic electrogenerated chemiluminescence (ECL) based assay was reported to detect the infection biomarker, CRP by covalently attaching synthetic ssDNA and CRP on Au(111) electrodes using tris(2,2‘-bipyridyl)ruthenium(II) (Ru(bpy)32+) labels (Fig. 8).[95] This report demonstrated that ECL peak intensity was linearly proportional to the analyte CRP concentration over the range 1−24 µg/mL on anti-CRP-Ru-(bpy)32+ modified Au working electrode.[95] Detection of CRP and *Mycobacterium tuberculosis* lipoarabinomannan (LAM) as infection biomarkers has been reported using a SiN nanophotonic lab-on-a-chip platform.[97] This sensor chip contained multiplexed Mach–Zehnder interferometers with an on-chip optical spectral analyzer composed of an arrayed-waveguide grating and integrated with a polymer microfluidic cartridge. This PoC based platform demonstrated CRP detection with LOD of 19.478 ng/mL.

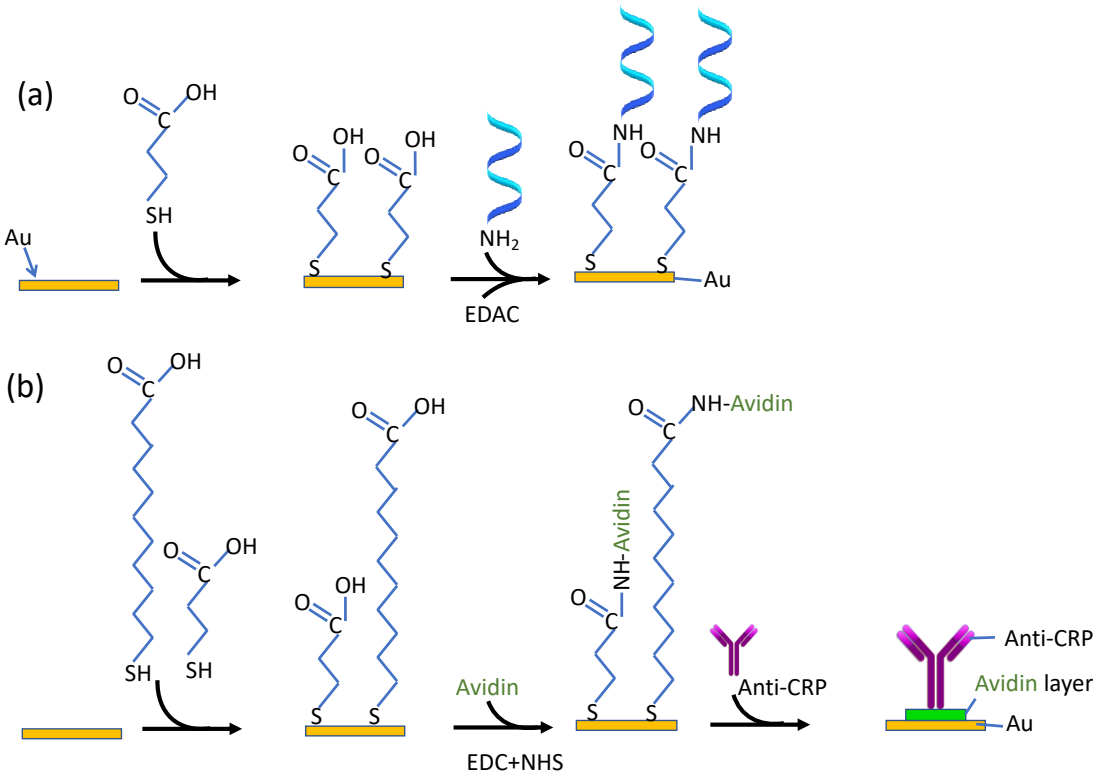

Fig. 8. Schematic diagram of; (a) immobilization of ssDNA probe onto the surface of Au(111) with linker 3-mercpatopropionic acid monolayer; and (b) immobilization of anti-CRP on Au(111) surfaces with varying lengths of alkane thiol linkers and avidin layer that essentially keeps surface immobilized molecules at different distances from the Au-surface.[95]

View Article Online
DOI: 10.1039/D0AN00896F

A bright-field imaging plasmonic biosensor was developed for biomarker detection such as biotinylated bovine serum albumin (bBSA) and human C-reactive protein (CRP), a clinical biomarker of acute inflammatory diseases. Here, gold nanohole based micro arrays were fabricated using standard UV-lithography combined with ion beam etching method (Fig. 9a). This sensor capable of generating heatmaps images which could locate the single nanoparticles with contrast spikes (Fig.9a-c). This method demonstrated sensitivity and limit of detection (LoD) of 10 pg/mL for bBSA and 27 pg/mL for CRP.

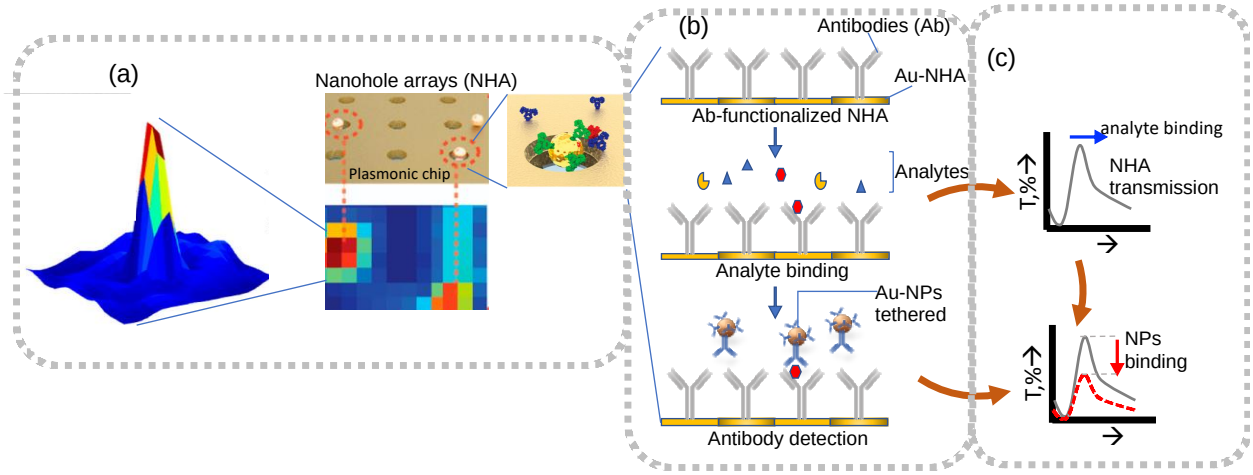

Fig. 9. Nanoparticle-enhanced plasmonic imager for digital biomarker detection. (a) bright-field image of a plasmonic biosensor that allows visualizing of single subwavelength Au-nanoparticle on large NHA area; (b) Au-NHAs and biomolecule binding and; (c) Simulated transmission spectrum based spectral shifts in peak positions before and after NPs binding.[101]

A phase-sensitive interferometer based optical PoC biosensor has been used for the detection of CRP, IL6 and miRNA-16 in a label-free and microarrays-type of configuration.[102] The sensor chip in this biosensor utilizes metallic nanostructures that transduces signal with specificity and LOD of 18 µg/mL, 88 µg/mL and 6 µg/mL for CRP, IL6 and miRNA-16, respectively in individual assays.[102] In another study, a PoC testing platform with gas generating reaction mediated biosensor is developed by combining principles of ELISA and lateral flow-type immunochromatographic strips (ICS) [133]. This PoC method utilizes antibody conjugated Au@Pt core/shell nanoparticles (Au@PtNPs) similar to AuNPs. Presence of PtNPs on AuNPs makes it reacts with H_2O_2, while the embedded antibodies interacts with CRP and generates O_2 corresponding to level of CRP present in the reaction. The released O_2 drives the pre-existing blue ink by capillary force in the ICS, making it visible to naked eye with LOD of 0.041 µg/L.[133]

View Article Online
DOI: 10.1039/D0AN00896F

A filter paper based colorimetric immunosensor found to be a less-expensive material for developing sensors. The paper-based sensing often rely on plasmonic gold nanoprobes for detection of analytes, such as IL-6.[106] Such type of sensing carried out by sandwich immunoassays that undergo three bio-conjugation routes for protein attachment to gold nanoprobes. These nanoprobes have to be first pre-activated to generate free -COOH or NH_2 functionalities or polyvinylpyrrolidone (PVP), and utilize alternating layers of polyelectrolytes to bind the capture antibody to the paper substrate (Fig. 10). These sensors can be coupled with smartphones to capture images as well as use them for computing the signals, if undetectable to naked eye. The embedded smartphone algorithm can also be used to quantify diagnostic signal corresponding the levels of target analyte/biomarker present in the test sample. In one case, for instance detection of IL-6 is made with a LOD as low as 0.1 pg/mL within 17 min. This type of smartphone based plasmonic detection of infections is most suitable for PoC testing in remote settings.

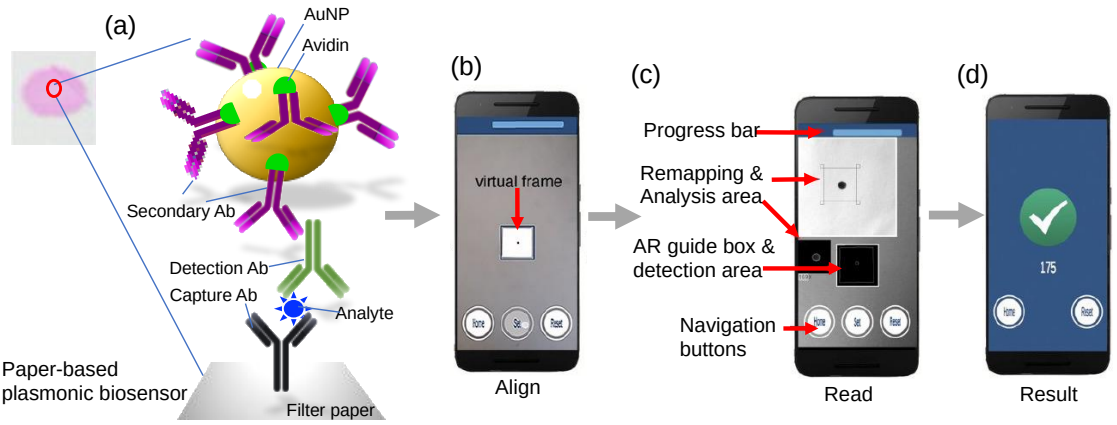

Fig. 10. Schematic representation of the plasmonic mobile biosensors (a-b) Antibody-decorated gold nanoparticles generate colored spots and quantified with smartphone, (c-d) The detection screen appears shows detecting region and results output is displayed.[106]

A unique magnetic immunoassay three dimensional optics biosensor has been developed which utilizes total internal reflection magnetic imaging (TIRMI) for PoC detection of C-reaction protein (CRP) [107] (Fig. 11). The chip was fabricated using a prism-like 3D glass substrate and a polymethyl methacrylate (PMMA) substrate surface on which micro channel was patterned (Fig. 11a). Here, the signal is generated from total internal reflection similar to that of SPR phenomenon when capture particles sandwiched with target analyte on the surface. The device is coupled with a CCD camera that captures the reflected light and the changes in the total internal reflection is recorded. The magnetic immunoassay on chip based on TRIMI principle demonstrated the detection limit of 0.1 ng/mL for CRP in buffer (Fig.11b). This type of

View Article Online
DOI: 10.1039/D0AN00896F

new transducers are although promising for PoC diagnosis of infection, but required further improvement, iteration and testing with large number for real biological samples.

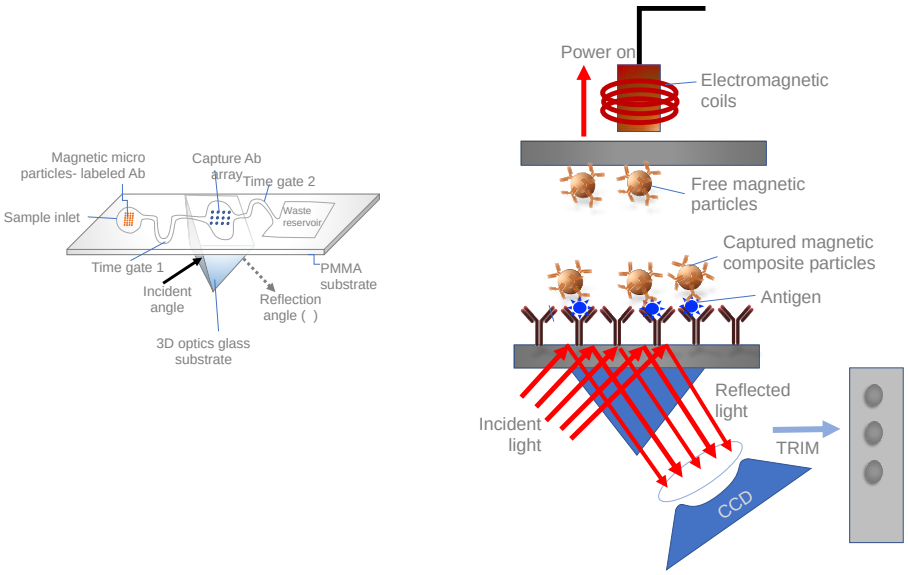

Fig. 11. (a) The design of the disposable microfluidic biosensor chip and (b) schematic of the measuring principle for the biosensor.[107]

A number of other studies have been reported on development of optical sensors for the detection of infection biomarker (PCT), such as a fluorescence immunoassay for a TIRF (total internal reflection)-based PoC testing device.[121] This method was based on generation of evanescent waves, which specifically excites fluorophores that bound previously on the surfaces, while the signals from sandwiching reactions were measured. This type of PoC based biomarker detection exhibited remarkable sensitivity with LOD of 0.04 ng/mL for PCT. Another study reported on molecular imprinted SPR biosensor which utilizes sensor surface carrying molecular imprints to bind PCT molecules.[122] This sensor exhibited LOD of 9.9 ng/mL PCT within ~1 h in simulated blood plasma. Other SPR based immunoassays that have been developed for real-time infection detection with PCT showed dynamic detection range from 4–324 ng/mL with LOD of 4.2 ng/mL and limit of quantification (LOQ) of 9.2 ng/mL.[123] Fiber optic sensors also function similar to SPR principle and presents convenient and flexible configuration with which nanogold-linked immunosorbent assay have been conducted. Sensitive detection of PCT by fiber optic sensor is reported and demonstrated a wide linear response range from 1 pg/mL to 100 ng/mL with extremely low LOD of 95 fg/mL (7.3 fM) for PCT (analysis time ≤15 min).[130] Other notable optical sensors include electrochemiluminescent immunosensor which is found to be most sensitive for detecting PCT that is mediated by CdTe quantum dots enhancement and specific-nanobodies and demonstrated PCT detection with LOD of 3.4 pg/mL. Here, CdTe quantum dot encapsulated silica

View Article Online
DOI: 10.1039/D0AN00896F

nanoparticle tags were utilized to assist signal amplification with nanobodies on to a chitosan–graphene nanocomposite modified glassy carbon electrode.[127]

Optical sensing platforms have been further improved in terms of sensitivity which is most suitable for detecting trace amounts of clinical samples. For instance, atto-molar to femto-molar CRP detection by molecular switching fluorescence based assay combined with total internal reflection microscopy.[110] Rapid diagnosis of infections is most likely accompanied by a sensitivity tradeoff, such as for detection of CRP using thin polymer/aptamer films fabricated onto the optical fiber device that distinguished between pathological (20 mg/L of CRP) from non-pathological concentration (2 mg/L CRP) within 15 min.[111] Similar tradeoff also applies to nitrocellulose based sensors, for e.g., a metal clad leaky waveguide (MCLW) sensor for detecting CRP in a diluted real serum sample by using nitrocellulose coated on a sensor chip.[112] Improvement in nitrocellulose based sensors have been attempted, where lateral flow assay (LFA) based tests were coupled with fluorescent CdSe/ZnS quantum dots (QDs) nanospheres instead of conventional Au-based LFAs. For instance, employing a immunofluorescent nanospheres (IFN) each made of 332 ± 8 CdSe/ZnS QDs gave rise to 257-fold more sensitivity for detecting infection using target CRP, which is unlikely to achieve with conventional Au-based LFAs. Fig. 12 shows the configurations of CdSe/ZnS nanosphere-based test strip and illustrated detection method for CRP detection using IFN-based test strip. The developed sensor test strip demonstrated CRP LOD of 27.8 pM.[113]

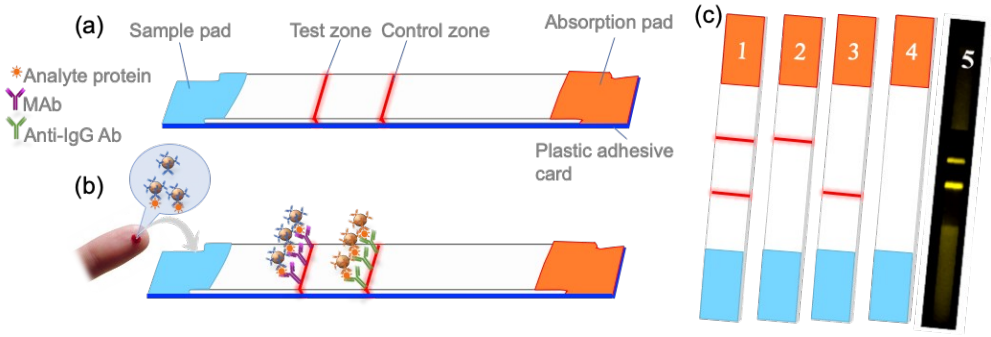

Fig. 12. Schematic illustration of; (a-b) the configurations of immunofluorescent nanospheres (IFN)-based test strip similar to conventional lateral flow strip assays expect that in place of Au-nanoparticles, CdSe/ZnS quantum dot (QD) nanospheres were used. (c) Schematic interpretation of 1) positive, 2) negative, 3-4) invalid and 5) after excitation of QDs showing the sensitivity of signal for the detection of CRP using IFN-based test strip.[113]

In another study, CRP detection was attempted using a smartphone-based colorimetric biosensor platform. This platform utilized graphene nanoplatelets (GNPs) for covalent attachment of specific antibody that provided signal enhancement. This sandwich assay demonstrated a wide linear range of

View Article Online
DOI: 10.1039/D0AN00896F

0.03–81 ng/mL with a LOD of 0.07 ng/mL in diluted human whole blood and plasma.[120] Buchegger et al. (2012) demonstrated PoC based detection of multi-analyte infection biomarkers, such as IL-6, IL-8, IL-10, TNF alpha, S-100, PCT, E-Selectin, CRP and Neopterin by fluorescence microarray scanning assay that utilizes streptavidin coated magnetic particles.[116] The sensitivity of this sensor is remarkable with picogram to nanogram per mL. Other biochemical-immunological hybrid biosensor include two-dimensional (2-D)-chromatography for the multi-analyte biomarker detection such as CRP, PCT and lactate.[117] This hybrid sensor is a good example for the advancement in lateral-flow type sensors, where combination of enzymatic and immunological reactions were employed for detection on lateral flow-strips. Here, an enzyme-reaction zone on the signal pad of typical immuno-strip was integrated for the rapid quantification on a smartphone-based detector.[117]

Further, localized surface plasmon resonance (LSPR)-based microfluidic optical chip sensor is fabricated for detection of six cytokines, such as IL-2, IL-4, IL-6, IL-10, TNF-α, and IFN-γ for monitoring of infections.[131] The chip comprised of microarrays of Au nanorods (AuNRs) integrated with microfluidic channels (Fig. 13a-c). The SEM images of sensor chip in Fig. 13a shows histograms of the particle-to-particle distance of the AuNRs. When analyte samples were introduced on to antibody-functionalized AuNRs, it induces a redshift and scattering intensity change of the longitudinal SPR.[131] The LOD determined using this method is achieved in 1-20 pg/mL range for six cytokines, such as IL-2 (20.56 pg/mL), IL-4 (4.60 pg/mL), IL-6 (11.29 pg/mL), IL-10 (10.97 pg/mL), TNF-α (11.43 pg/mL), IFN-γ (6.46 pg/mL) within 40 min is a significant advancement in optical biosensing.

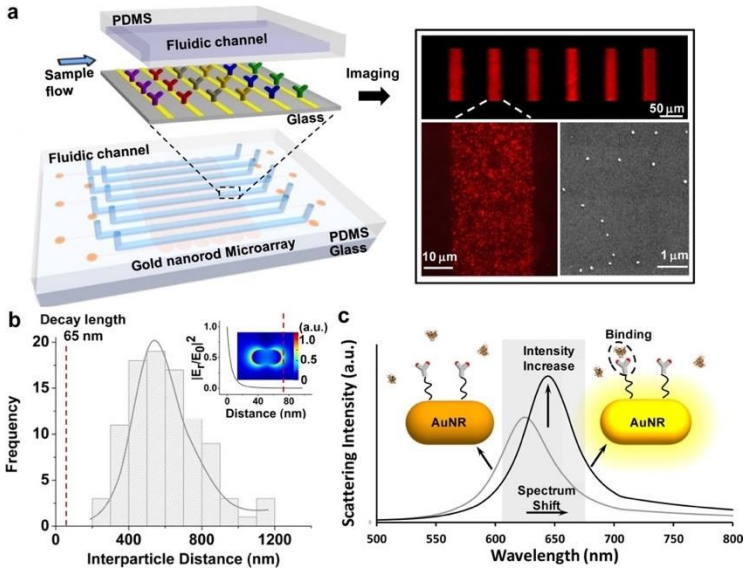

Fig. 13. (a) Schematic illustration of the LSPR AuNRs nanoplasmonic chip containing microarrays and its appearance in SEM image, (b) Histograms of the particle-to-particle distance of the AuNR arrays on chip and the inset figure shows simulated intensity profile of single AuNR excited by incident light, and

View Article Online
DOI: 10.1039/D0AN00896F

(c) The principle of the method demonstrating capture of analyte by antibody-functionalized AuNR LSPR biosensor results in a redshift and scattering intensity change of the longitudinal SPR.[131]

5.2. Electrochemical-biosensing platforms

Electrochemical biosensors have received considerable attention for detecting infection biomarkers. These electrochemical biosensing schemes utilize a variety of intermediary chemical agents, such as nanoparticles, polymer thin films (membrane), nanotubes, nanohybrids and synthetic molecular probes to demonstrate bacterial and viral biomarkers detection. Following are some of the unique electrochemical biosensor schemes that has been reported for detection of infection biomarkers.

A smartphone-based label-free electrochemical WBC counting device is developed using microporous paper with patterned gold microelectrodes.[43] This WBC counting sensor design and principle is presented in Fig.14a-f. Here, polyvinylidene fluoride (PVDF) membrane with microfabricated interdigitated electrodes and analytical ion probes (ferricyanide/ferrocyanide) were used for electrochemical quantification of WBC (Fig.14b-c). Authors reported efficient trapping of WBC on sensor electrode that was facilitated by the porous property of the membrane electrodes providing sufficient charge transfer property that can be tracked by differential pulse voltammetry (DPV). Here, DPV measurement is made with a coupled handheld smartphone through wireless Bluetooth communication and demonstrated its applicability for PoC applications. The dynamic detection range of this electrochemical sensor covers WBC count of 200–20000 μL^{-1} with 10 μL sample with high reproducibility.

View Article Online
DOI: 10.1039/D0AN00896F

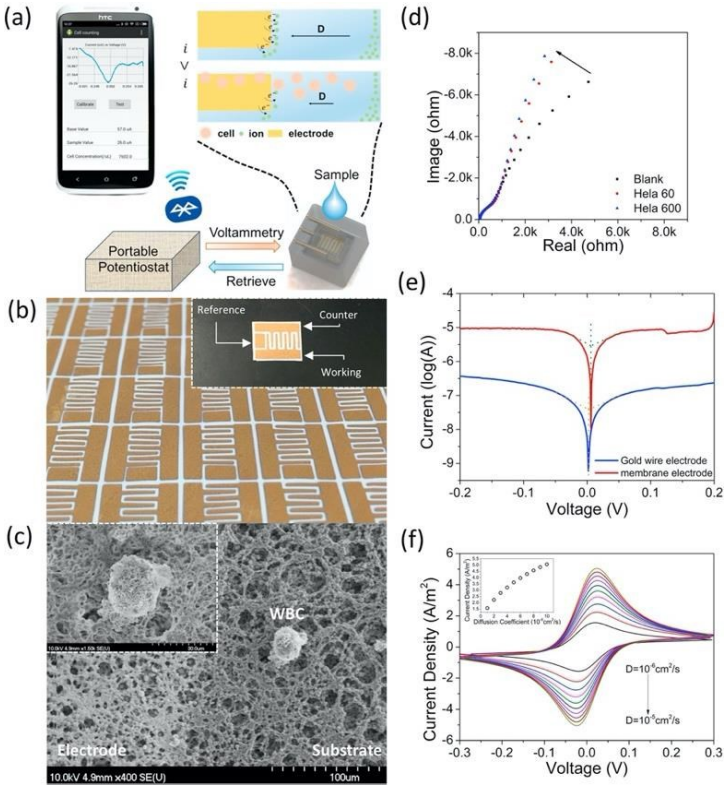

Fig. 14. (a) Electrochemical WBC counting sensor device design and principle; (b-c) microporous paper with patterned gold microelectrodes-three electrode electrochemical sensor on microporous PVDF membrane paper and SEM image of trapped WBC on sensor. (c-f) Nyquist plot (with Hela cells frequency sweep-10 Hz to 100 kHz), Tafel plot and cyclic voltammetry responses of electrochemical sensor in different diffusion coefficient in the 1 mM $[Fe(CN)_6]^{3-}/[Fe(CN)_6]^{4-}$ environment.[43]

One of the alternative approaches taken to detecting WBCs is impedance cytometry and velocimetry, which is also applicable to RBCs. In one study, microfluidic chip is developed for the screening of WBCs and RBCs.[93] This chip utilizes a polyelectrolyte salt bridge-based electrode (PSBE) and work on a coulter counter principle. PSBEs in the chip configuration were electrochemically connected to an external dc impedance analyzer through isotonic NaCl and Ag/AgCl electrodes. Signal acquisition from microfluidic chip is based on the dc impedance changes (Fig. 15a-b). By keeping bias voltage (0.4-V dc) and current (~13-µA dc) steady, the impedance signals responds to the cells or microbeads passing through the microchannel between the PSBEs and converted to amplified voltage signal screening rate of over 1000 cells/s and a velocity of the cells of over 100 mm/s within 1 h (Fig. 18b).

View Article Online
DOI: 10.1039/D0AN00896F

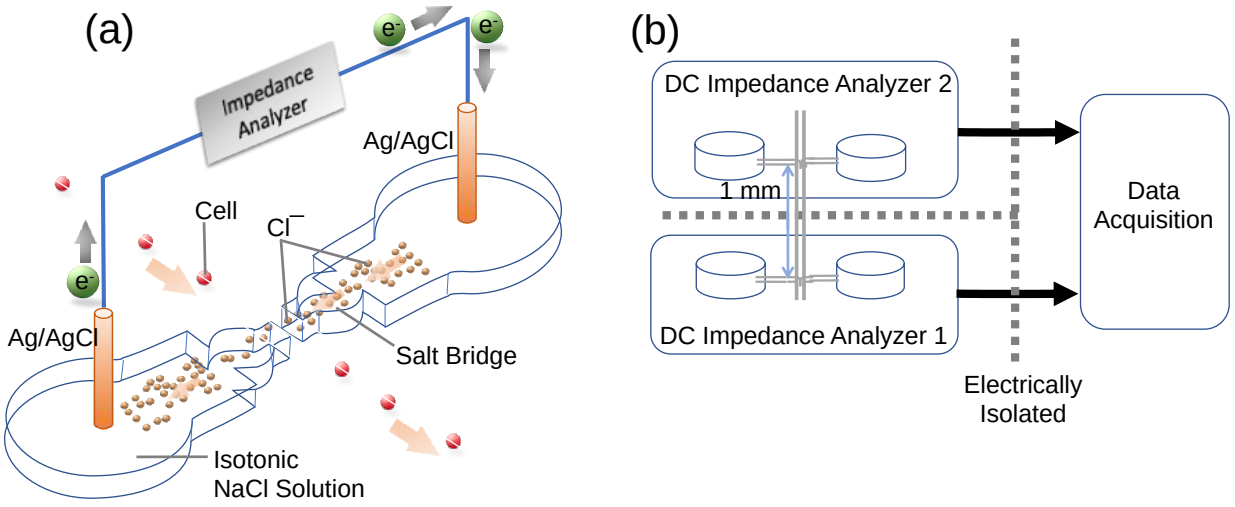

Fig. 15, (a) DC impedance analysis of the microchannel with the PSBEs and showing Ag/AgCl electrodes that were electrochemically connected to two PSBEs through an isotonic NaCl solution under applied dc bias (0.4V). (b) The data acquisition for velocimetry chip of two pairs of PSBEs and electrically isolated to eliminate potential cross-talk.[93]

Further advancement in microfluidics integration and portability has been reported by Furniturewalla et al. (2008), where a fully integrated flexible wearable microfluidic impedance cytometer system was developed to obtain generalized blood cell counts and tested RBCs and WBCs.[134] This system consists of polydimethylsiloxane (PDMS) microfluidic channels coupled with a transduction signal circuit using customized microcontroller made of an 8-bit analog-to-digital converter (ADC), lock-in-amplification (LIA) system and a Bluetooth module that fit on a wristband (Fig. 16a-b). The designed LIA with ADC demonstrated detection of particles as small as 2.8 μm (Fig. 16b). Although, this may not be bio-specific but essentially could replace traditional microscopic methods used for counting cells.

View Article Online
DOI: 10.1039/D0AN00896F

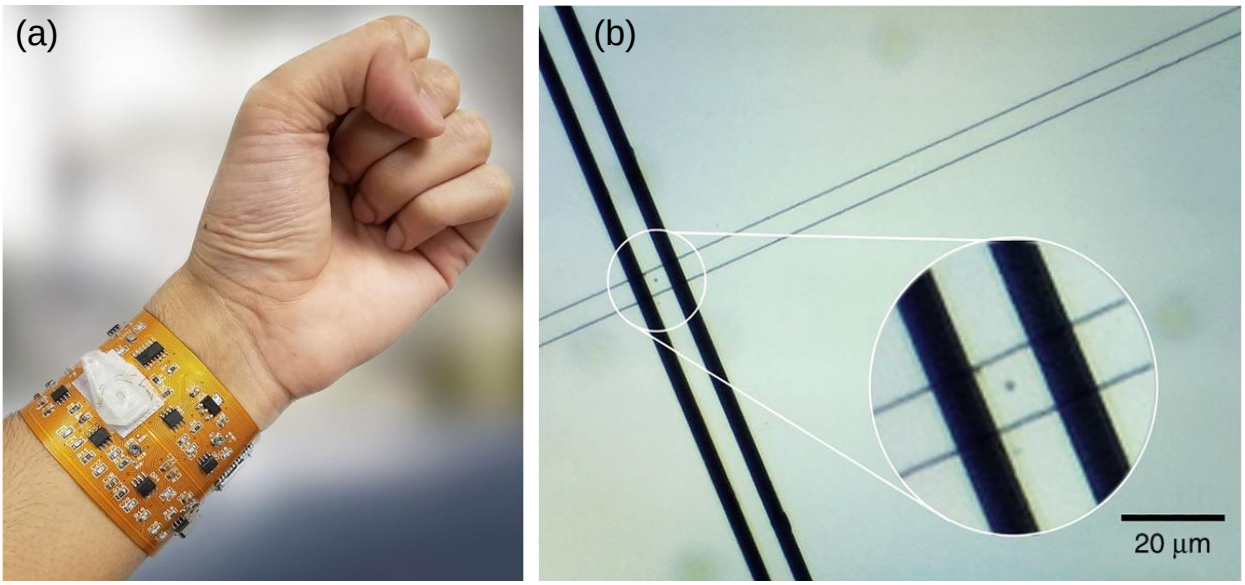

Fig. 16. (a) Wearable microfluidic impedance cytometer system on flexible substrate and (b) top view of 30 µm microfluidic PDMS channel pore with sheep blood cells shown flowing across electrodes.[134]

Further improvement has been made in regard to detecting blood particles by combining electrical and optical methods in which a PoC cytometer is integrated with smartphone and microfluidic chips for counting particles (blood). Similar studies were recently reviewed that were more focused on PoC device system development for counting of blood particles, such WBCs and RBCs and these were mainly grouped in opto-fluidic cytometer, impedance cytometer and imaging cytometer and all these are applicable to detection of infections.[135]

Erythrocyte sedimentation rate (ESR) has been used an indicator of infection. The Westergren method is simple, standard and widely used for measuring the ESR in plasma samples. The ESR measurement is made in terms of its height in mm from the plasma supernatant in a vertically mounted pipette following 1 h blood sedimentation.[136] Here, minimum sedimentation scale is 200 mm and minimum bore of 2.55 mm. In order to minimize the time of ESR test, several attempts have been made to develop direct and indirect method to shorten the ESR test time. Detailed literature related to such approaches can be found in previous reports,[94] where a new approach based on electrochemical sensing has been employed that correlated blood conductivity and sedimentation that shorten the ESR rate test. Rapid determination of ESR can be made using two planar electrodes-based and optical observations (Fig. 17 a-c). The sensing method in this ESR test is based on the change in conductivity of blood which is directly dependent on gravitational sedimentation of erythrocytes. This study showed blood sedimentation curve and hematocrit

View Article Online
DOI: 10.1039/D0AN00896F

profiles can be obtained in first 400 seconds of the recorded changes in blood conductivity, enabling measurements of the erythrocyte aggregation, as well as sedimentation kinetics.

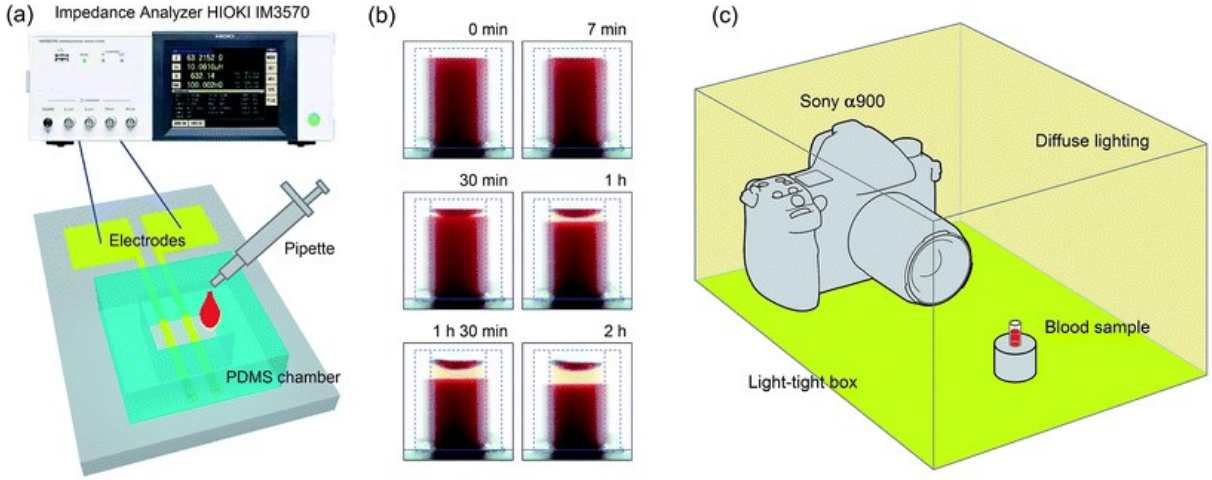

Fig. 17. (a) Electrical measuring system based on two planar electrodes electrochemical sensor and (b-c) optical observation of blood sedimentation using digital camera inside a light-tight box.[94]

As an infection and inflammatory biomarker, CRP has been a target for detection on many electrochemical sensors and one of the sensitive methods utilizes a biomimetic 3,4-ethylenedioxythiophene (EDOT) derivative bearing a zwitterionic phosphorylcholine group.[99] This sensor exhibited a LOD for CRP of 37 nM with a dynamic range of 10–160 nM. Other studies employed non-Faradaic electrochemical sensor for detecting dual PCT and CRP markers using zinc oxide thin film that requires an ultra-low sample volume of 10 µL.[100] The developed biosensor transduction mechanism relies on specific biomolecular interactions between the target analyte and the capture probe. This interaction is quantified accurately through changes in specific frequency by non-Faradaic-electrochemical impedance spectroscopy (EIS). LOD for PCT and CRP by EIS may not be comparable to other sensitive methods, however there is a trade-off in EIS being a label-free method. In another study, PCT and CRP biomarkers were detected by magnetic bead based immunoassay on screen-printed electrochemical sensor electrode.[103] This assay demonstrated high sensitivity with LOD 0.09 ng/mL and 0.008 µg/mL for PCT and CRP, respectively using low sample volumes (<30 µL) and under 20 min of total assay. Further, an electrochemical sensor based on synthetic peptides is developed in which synthesized peptides with cysteine residues at the C-terminus facilitated the thiol assembly for conjugation chemistry with protein that exhibited binding constant, K_d of 0.39 ± 0.11 nM for PCT BP3 peptide.[104]

View Article Online
DOI: 10.1039/D0AN00896F

Other unique electrochemical approaches for detecting infection biomarkers have been considered, such as that of electrochemical urine dipstick probe composed of molybdenum electrodes on nanoporous polyamide substrate to detected CRP and IL-6 in picogram/mL.[105] In one study, Cu/Mn doped CeO_2 nanocomposite (CuMn-CeO_2) has been employed as signal tags and amplifiers for fabricating an electrochemical immunosensor for detecting of PCT.[124] In this method doping of Cu, Mn into CeO_2 lattice structure generated excess oxygen vacancies and enhanced the redox and catalytic performance, making the sensor more responsive to a wide linear range of 0.1 pg/mL to 36.0 ng/mL with a LOD of 0.03 pg/mL. Other notable electrochemical immunosensors utilized ferrocene-modified Au nanoparticles for procalcitonin (PCT) detection with linear detection ranges for PCT between 1.5 pg/mL and 50 ng/mL with LOD of 0.8 pg/mL,[125] and PtNP-ferrocene carboxylic acid (Fc)-C60 nanocomposites with LOD of 0.01–10 ng/mL a detection limit of 6 pg/mL. Electrochemical sensitive detection of PCT is reported using C60 carboxyfullerene-based functionalized nanohybrids as signal-amplifying tags.[126] Selvam et al. (2017) developed an electrochemical biosensor for multiple infection biomarkers that include PCT, lipoteichoic acid (LTA), and lipopolysaccharide (LPS) which utilized nanoporous nylon membrane integrated onto a microelectrode sensor and achieved LOD of 0.1 ng/mL with PCT and 1 µg/mL for LPS and LTA.[128]

A significant advancement in electrochemical sensors is later made by combining unique features of reduced graphene oxide (rGO) nanomaterials and ELISA-like assays. Here, conducting rGO nanosheets/gold nanoparticles (rGO-AuNPs) nanocomposite increased the reaction sites due to high surface-to-volume ratio, enhancing the π-π conjugation capacity and surface conductivity. These nanostructures on the electrode surface absorb more capture antibodies (Ab1) and used for a sandwich-type electrochemical immunosensor by coupling with gold nanoparticles-enhanced tyramide signal amplification (AuNPs-TSA) for the detection of PCT [129]. Sensitive signal generation was then possible following reaction with Au NPs-horseradish peroxidase (HRP)-PEG-Ab2 conjugated to specific anti-PCT as shown in Fig. 18. The developed electrochemical immunosensor achieved a wide dynamic detection range from 0.05 to 100 ng/ mL and with LOD of 0.1 pg/mL.

View Article Online
DOI: 10.1039/D0AN00896F

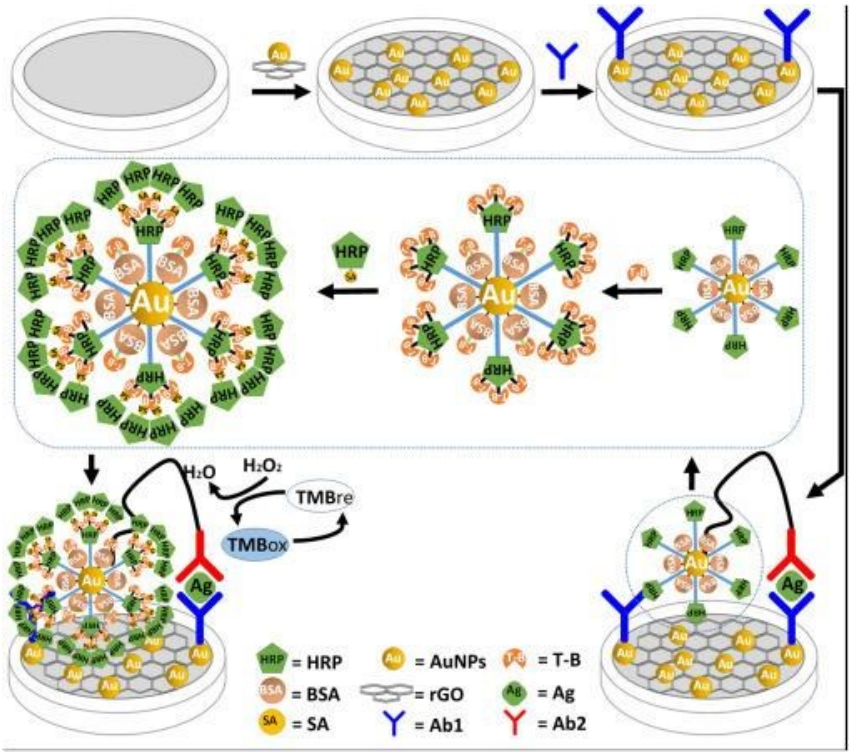

Fig. 18. Scheme showing fabrication of a sandwich-type electrochemical immunosensor for detection of procalcitonin (PCT).[129] Here, the sensor surface is modified with a nanocomposite of rGO-AuNPs as efficient carriers for primary antibodies (Ab1) while another antibody (Ab2) conjugated to a signal generating nanocomposite structure composed of AuNPs coated with horseradish peroxidase (HRP) enzyme (AuNPs-HRP-PEG-Ab2) which specifically bind to PCT antigen captured on sensor and generates sensitive HRP mediated electrochemical signal in presence of a redox mediator (TMB, 3,3′,5,5′-tetramethylbenzidine). The presented immunosensor based on rGO-AuNPs modified on electrode with high surface-area-to-volume ratio, enhanced conductivity and also π-π conjugation capability along with AuNPs-HRP-PEG-Ab2 nanocomposites with high stability and biological compatibility that greatly enhanced current signal in sensitively detecting PCT.

An electrochemical aptasensor later developed that essentially replaced use of antibodies for simultaneous detection of TNF-α and IFN-γ (interferon-gamma) by synthesizing respective linking aptamers to protein biomarkers.[137] The aptasensor exhibited a wide linear range and LOD for TNF-α with 9 to 88 ng/mL and 5.46 ng/mL, respectively. Whereas, aptasensor showed linear response for IFN-γ with 9-130 ng/mL and LOD of 6.35 ng/mL. However, sensitivity with aptamers under dynamic assay conditions in which they are not trained or adaptable to varying ionic strengths and physico-chemical nature of medium/test solution is a subject of further investigation.

View Article Online
DOI: 10.1039/D0AN00896F

5.3. Miscellaneous biosensing platforms

Apart from optical and electrochemical biosensing platforms, several other important sensing methods have been employed that aimed at detection of bacterial/viral infection related host biomarkers (WBC, CRP, TRAIL, IP-10). Sensors with notable and unique features in respect of detecting infection biomarkers are presented below.

Fourier-transform infrared (FTIR) spectroscopy has been demonstrated as a powerful tool to measure WBC to diagnose bacterial and viral infections using small samples of blood from patients.[138] Infrared microscopy has the capability to distinguish minor molecular and chemical changes in blood components. These changes occur upon secretion of biomarkers in the bloodstream combined with changes in the WBC and plasma structure (e.g., protein and carbohydrate structures) and provide a signature that enables diagnosing the etiology of human infection and infection type.[139] This method demonstrated possibility of identifying the infectious agent as bacterial or viral type based on infrared spectra of WBC combined with multivariate principle component analysis (PCA) followed by linear discriminant analysis (LDA) using control (normal) and test specimens that exhibit 82% for sensitivity and 80% for specificity within 1 h blood sample collection.[138] Another study reported leukocytes measurement using infrared spectra for rapid diagnosis of infection etiology in febrile pediatric oncology patients.[140] The above study hypothesized that the FTIR spectroscopy can be used to monitor viral and bacterial infections as a result of biochemical changes in leukocytes occurred by different responses of the human immune system against viral and bacterial infections. The FTIR spectral changes from leukocytes for control, bacterial and viral infections combined with their classification using machine learning algorithms can be used to diagnose the etiology of infection as bacterial or viral within 70 min of the blood sample collection with 93% sensitivity and 88% specificity.[140] It is clear that infrared spectroscopy is a promising new method for the diagnosis of bacterial and viral infections, however its applicability under PoC settings still remains to be explored.

A PoC giant magnetoresistive (GMR) sensor chip is utilized to perform multiplexed detection of multiple analytes, such as for human immunodeficiency virus (HIV) or leukocytosis.[92] It is reported that leukocytosis is a condition of elevated WBCs and that the neutrophil count is highly correlated with WBC count. Therefore, detection of neutrophil elastase (NE) levels in plasma serve as an indicator of leukocytosis. The PoC GMR sensor chip system comprised of an array of magnetic sensors combined with superparamagnetic iron oxide nanoparticles (SPIONs) for detection of HIV in saliva and leukocytosis in plasma and whole blood. GMR sensor detection is based on sensitive changes occur as a result of local magnetic field of SPIONs corresponding to analyte concentration. In this PoC system, each diagnostic chip consisted 80 individual magneto-nanosensors that can perform multiplexed detection of

View Article Online
DOI: 10.1039/D0AN00896F

multiple analytes in a single sample. Each chip was wire-bonded to printed circuit board (PCB) along with smartphone application for operation and guidance to facilitate self-testing of PoC device (Fig. 19). The sensor chip demonstrated HIV in saliva with an accuracy of 80% and leukocytosis in plasma with an accuracy of 90% that has a great potential to be expanded to a range of other disease biomarkers or living cells.[92]

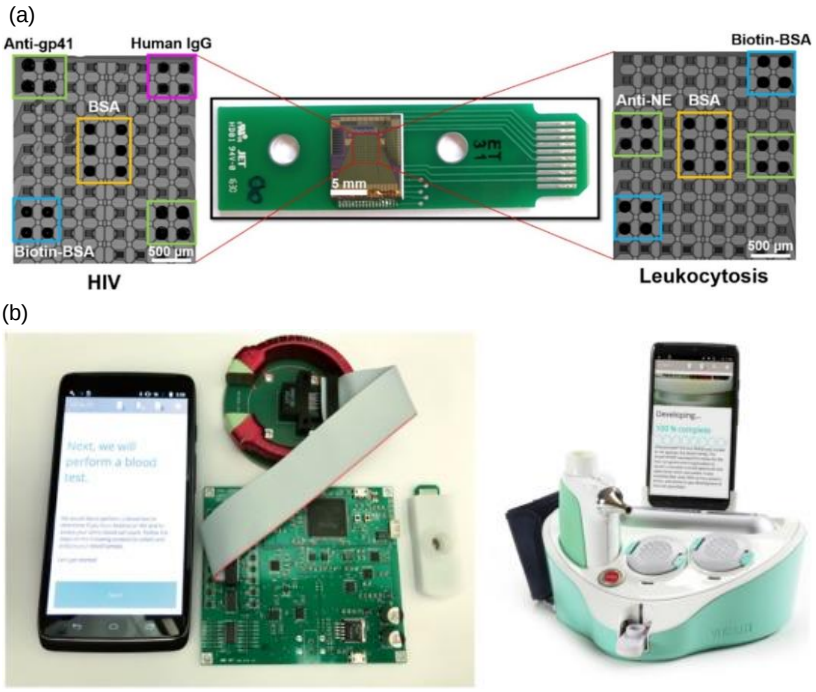

Fig. 19. (a) Giant magnetoresistive (GMR) nanosensor chip on printed circuit board (PCB) and spotted sensor array for HIV and leukocytosis detection and (b) Integrated GMR nanosensor diagnostic platform that includes a disposable cartridge, a processor station, and a smartphone.[92]

A similar detection principle is reported in which a flexible giant magnetoimpedance (GMI)-based biosensor is used for the detection of CRP. This platform is made of a gold film coated over a cobalt-based amorphous ribbon (Metglas® 2714A) that served as a transducer as well as a support for the immuno-platform (Fig. 20a and b). This sensor utilizes a sandwich assay regime and detected CRP by change in resistance with a detection range between 1 to 10 ng/mL.[96]

A PoC platform based on a nanogap-embedded field effect transistor (FET) has been used for CRP detection in serum that exhibited a detection range of 0.1 ng/mL to 100 ng/mL [118]. Acoustic based sensor has been employed in immunoassay such as Resonant Acoustic Profiling™ (RAP™) for detection of inflammation and infection using CRP as a biomarker with lower limit of detection by homogenous and direct sandwich assay with a detection range of 3 to 20 ng/mL.[98]

View Article Online
DOI: 10.1039/D0AN00896F

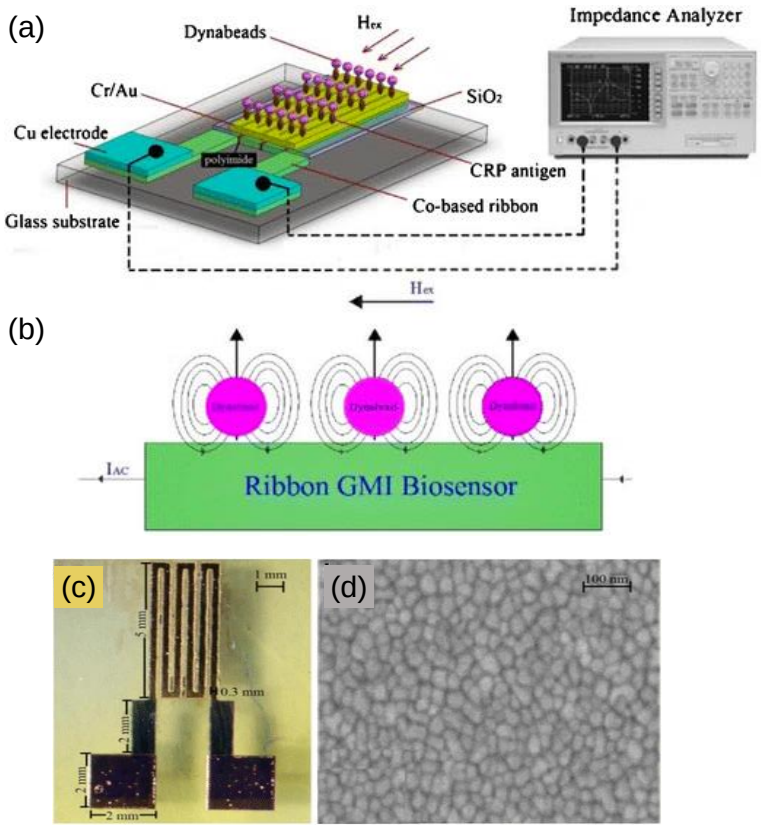

Fig. 20. (a) Graphical illustration of CRP test setup. (b) Magnetic field arrangement of the beads under an applied magnetic field [96]. (c) The top view of fabricated GMI biosensor and (b) The nano-gold film serves as the immune platform.[96]

According to the latest development, only one study reported on a new assay called ImmunoXpert assay, which relies on laboratory equipment and require trained personnel to conduct the assay. ImmunoXpert assay is not yet widely tested however, it is potentially be used for differentiating between viral and bacterial infections. This assay utilizes three protein biomarkers, such as virus-induced tumor necrosis factor related apoptosis inducing ligand (TRAIL), interferon-gamma-induced protein-10 (IP-10 or CXCL10), and bacteria-induced CRP.[37, 38, 83] In addition to biosensor development for infection biomarkers detection, few of selected diagnostic technology development with FDA approval status has been reviewed for bacterial LRTIs summarizing development of modality such as matrix-assisted laser desorption/ionization time-of-flight mass spectrometry (MALDI-TOF MS), serological tests, and urine antigen tests for LRTIs.[50] However, rapid, near the patent-bed side PoC biosensor system testing for differential diagnosis of viral and bacterial infections could prevent false diagnosis or misuse of

View Article Online
DOI: 10.1039/D0AN00896F

antibiotics and also prevent antibiotic resistance which necessitates the future directions on developing PoC based systems.

6. Conclusions and perspectives

It is crucial to differentially diagnose bacterial and viral diseases at early stages of their progression, which allows successful treatment and recovery of patients. Therefore, it is essential to develop simple and sensitive diagnostic methods that can rapidly detect multiple bacterial and viral biomarkers at very low concentrations in biological fluids. Currently, bio-sensing technology platforms can meet these demands, but most of these rely on single or diverse biomarker types not designed for differentiating viral/bacterial infections. Most of the sensitive detection schemes are time-consuming or require sophisticated laboratory equipment and training. In addition to selecting a sensitive transducer platform, choice of target host multiple biomarker panel becomes extremely important for not only detecting infections, but also differentially diagnose whether the infection is of viral or bacterial origin. In this review, we summarized bacterial and viral infection associated biomarkers, classical clinical methods and recently available biosensing platforms (microfluidic chip, paper platform, electrochemical and plasmonic chips, wearable sensor system) for bacterial and viral biomarkers detection. Most significant bacterial and viral biomarker/s for biosensing in preference order are identified as TRAIL > IP-10 > PCT > CRP > WBC > PMNs on optical, electrochemical and magnetic transduction formats. Additionally, vitamin D level is found to be a strong predictor of the immune response to bacterial and viral infections. However, further research trials are essential for vitamin D's diagnostic value as bacterial/viral biomarker as well as guiding therapy for viral URTIs. Myxovirus resistance protein A (MxA) and Heparin-binding protein (HBP) have also emerged as potential new biomarker targets for detection and differential diagnosis of viral and bacterial infections that remains to be explored for biosensing. Diagnosis of viral/bacterial infections using a specific biomarker is difficult. Therefore, combination of a range of biomarkers from Tables 2 and 3 can be considered for reliably differentiating viral or bacterial infections for making accurate clinical decisions.

A number of methods are available for detection of bacteria either directly or indirectly by using host biomarkers. Here, traditional immunoassays, such as ELISA is the most suitable, accurate and reliable method existed to date, but not suitable for PoC applications. However, such assays/kits although available in centralized laboratories but are expensive and require sophisticated laboratory and trained personal to run the tests. In order to find alternative approaches, this review went on to explore some of the detection methods used for detection of viral and bacterial infections by targeting host biomarkers or antibodies. Detection of viral infection by means of host biomarkers is not well established nor widely accepted, because majority of bacterial and viral biomarkers are also markers of common inflammation,

View Article Online
DOI: 10.1039/D0AN00896F

making it difficult to distinguish the specific type of infection risk. However, viral-specific host antibodies could serve as powerful targets provided that prior knowledge is available on specific virus to be detected. Assays can then be designed using the antibodies raised against the same virus particle or use antibodies against its surface-coat protein fraction (e.g., spike protein of SARS-CoV-2) for detection. The detection, however, can then be made using a sensitive immuno-sensing scheme.

A multiple marker detection strategy needs to be adapted using a combination of established and new potential bacterial and viral markers, which helps in making accurate clinical decisions. Recently, many of biosensing platforms have been developed by utilizing nanomaterials because of their extraordinary optical, electrical and magnetic properties with highly active functional surfaces, which are most desired features in biosensing technology application. Viral and/or bacterial infections can then be detected from host serum samples using specific antibodies in a PoC setting. Lab-on-a-chip electrochemical and fluorescence based biosensing platforms holds great promise in quantitative analysis mediated by active electrode nanomaterials (metal/metal oxide/carbon/hybrid) and optical nanomaterials (quantum dots, nanoparticles) for easy, simple and accurate results. These combined with unique features, such as (a) integration of multiple nanomaterial-based transducing arrays with microfluidic platform and (b) designing user-friendly read-out circuit and data-analysis unit, such as smartphone application is most essential for developing future PoC biosensing devices that enables early discrimination of bacterial and viral infections with speed and sensitivity.

Future directions in biosensing technology are more inclined toward developing less-expensive PoC tools for detecting and differentially diagnosing viral/bacterial infections, as well as extending these to other chronic diseases. Integration of highly luminescent QDs with unique emission profiles with PoC tools are emerging as promising features that provide distinctive optical signatures and sensitivity to PoC detection. Such distinctions in QDs' functionality not only enable detecting specific biomarker levels, but also multiplexing by which differentiation of viral and bacterial infections can be made with speed, sensitivity, specificity, portability and cost-effectiveness without having to rely on centralized laboratories or waiting for the test results.

Acknowledgements

We are grateful to our daughters Aisha and Aalia for their cooperation in our home office at times of COVID-19 pandemic.

View Article Online
DOI: 10.1039/D0AN00896F

References

1. WHO, Environmental factors influencing the spread of communicable diseases. https://www.who.int/environmental_health_emergencies/disease_outbreaks/communicable_diseases/en/, https://www.who.int/environmental_health_emergencies/disease_outbreaks/communicable_diseases/en/, (accessed April 12, 2020, 2020).
2. WHO, The top 10 causes of death. https://www.who.int/en/news-room/fact-sheets/detail/the-top-10-causes-of-death, https://www.who.int/en/news-room/fact-sheets/detail/the-top-10-causes-of-death, (accessed April, 12, 2020, 2020).
3. WHO, Influenza Laboratory Surveillance Information by the Global Influenza Surveillance and Response System (GISRS). https://www.who.int/influenza/surveillance_monitoring/updates/latest_update_GIP_surveillance/en/, (accessed April 12, 2020, 2020).
4. WHO, Rolling updates on coronavirus disease (COVID-19). https://www.who.int/emergencies/diseases/novel-coronavirus-2019/events-as-they-happen, https://www.who.int/emergencies/diseases/novel-coronavirus-2019/events-as-they-happen, (accessed April 12, 2020, 2020).
5. FDA, Factors Potentially Contributing to the Contamination of Romaine Lettuce Implicated in the Fall 2018 Multi-State Outbreak of E. coli O157:H7., https://www.fda.gov/media/120722/download, (accessed April 12, 2020, 2020).
6. C. f. d. c. a. Prvention, *2019 outbreaks: E. coli Infections*, 2019, https://www.cdc.gov/ecoli/2019/o2103-2004-2019/index.html.
7. N. H. S. N. England, *Mid Essex Clinical Commissioning Group*, 2019, https://midessexccg.nhs.uk/news/1057-group-a-streptococcus-outbreak-in-mid-essex.
8. E. C. f. D. P. a. Control, *Threats and outbreaks*, 2019, https://ecdc.europa.eu/en/publications-data/rapid-risk-assessment-ebola-virus-disease-outbreak-north-kivu-and-ituri-1.
9. E. Dong, H. Du and L. Gardner, *Lancet Infect. Dis.*, 2020, DOI: 10.1016/S1473-3099(20)30120-1.
10. WHO, Emergencies preparedness, response. https://www.who.int/csr/don/archive/year/en/, https://www.who.int/csr/don/archive/year/en/, (accessed April 12, 2020, 2020).
11. WHO, WHO Report on Surveillance of Antibiotic Consumption: 2016 - 2018 Early implementation. https://www.who.int/medicines/areas/rational_use/oms-amr-amc-report-2016-2018/en/, https://www.who.int/medicines/areas/rational_use/oms-amr-amc-report-2016-2018/en/, (accessed April 12, 2020, 2020).

View Article Online
DOI: 10.1039/D0AN00896F

12. D. Prilutsky, E. Shneider, A. Shefer, B. Rogachev, L. Lobel, M. Last and R. S. Marks, *Anal Chem*, 2011, **83**, 4258-4265.
13. O. Ortashi, J. Virdee, R. Hassan, T. Mutrynowski and F. Abu-Zidan, *BMC Med. Ethics*, 2013, **14**, 42.
14. Z. Yu, H. Jing, P. Hongtao, J. Furong, J. Yuting, S. Xu and P. Venge, *J. Immunol. Method.*, 2016, **432**, 82-86.
15. J. Nuutila, & Lilius, E.-M., *Cur. Opin. Infect. Dis.*, 2007, **20**, 304-310.
16. A. Qureshi, Y. Gurbuz and J. H. Niazi, *Sens. Act. B. Chem.*, 2012, **171**, 62-76.
17. C. S. Kosack, A. L. Page and P. R. Klatser, *Bull. World Health Organ*, 2017, **95**, 639-645.
18. Y. Z. Wang, L. Yu, X. W. Kong and L. M. Sun, *Int J Nanomed*, 2017, **12**, 4789-4803.
19. O. Pashchenko, T. Shelby, T. Banerjee and S. Santra, *ACS Infect. Dis.*, 2018, **4**, 1162-1178.
20. P. V. Dasaraju and C. Liu, in *Medical Microbiology. 4th edition*, University of Texas Medical Branch at Galveston, 1996.
21. V. R. Badhwar, S. Ganapathy, P. P. Prabhudesai, N. K. Tulara, A. Y. Varaiya and D. Vyas, *J. Assoc. Physicians India*, 2016, **64**, 95-101.
22. M. Hauptmann and U. E. Schaible, *FEBS Lett.*, 2016, **590**, 3721-3738.
23. G. C. Schild, W. D. Winter and C. M. Brand, *Bull. World Health Organ*, 1971, **45**, 465-471.
24. C. E. Taylor, *J. Clin. Pathol. Suppl. Coll. Pathol.*, 1969, **3**, 14-19.
25. M. C. Pierce, S. E. Weigum, J. M. Jaslove, R. Richards-Kortum and T. S. Tkaczyk, *Ann. Biomed. Eng.*, 2014, **42**, 231-240.
26. M. L. Y. Sin, K. E. Mach, P. K. Wong and J. C. Liao, *Expert Rev. Mol. Diagn.*, 2014, **14**, 225-244.
27. P. J. Tighe, R. R. Ryder, I. Todd and L. C. Fairclough, *Protem. Clin. Appl.*, 2015, **9**, 406-422.
28. A. Sosnik and M. Amiji, *Adv. Drug Delivery Reviews*, 2010, **62**, 375-377.
29. L. Syedmoradi, M. Daneshpour, M. Alvandipour, F. A. Gomez, H. Hajghassem and K. Omidfar, *Biosens. Bioelectron.*, 2017, **87**, 373-387.
30. O. N. Oliveira, Jr., R. M. Iost, J. R. Siqueira, Jr., F. N. Crespilho and L. Caseli, *ACS Appl. Mater.*, 2014, **6**, 14745-14766.
31. K. Stol, R. G. Nijman, W. van Herk and A. M. C. van Rossum, *Pediatr. Infect. Dis. J.*, 2019, **38**, S7-S13.
32. A. J. Kapasi, S. Dittrich, I. J. Gonzalez and T. C. Rodwell, *Plos One*, 2016, **11**.
33. A. Mohan and J. Harikrishna, *Indian J. Med. Res.*, 2015, **141**, 271-273.
34. S. S. Shah, L. Ambroggio and T. A. Florin, *J. Pediat. Infect. Dis. Soc.*, 2015, **4**, 189-191.

View Article Online
DOI: 10.1039/D0AN00896F

35. K. Oved, A. Cohen, O. Boico, R. Navon, T. Friedman, L. Etshtein, O. Kriger, E. Bamberger, Y. Fonar, R. Yacobov, R. Wolchinsky, G. Denkberg, Y. Dotan, A. Hochberg, Y. Reiter, M. Grupper, I. Srugo, P. Feigin, M. Gorfine, I. Chistyakov, R. Dagan, A. Klein, I. Potasman and E. Eden, *Plos One*, 2015, **10**.

36. B. D. Shepard and A. D. Badley, *Antiinfect Agents Med. Chem.*, 2009, **8**, 87-101.

37. I. Srugo, A. Klein, M. Stein, O. Golan-Shany, N. Kerem, I. Chistyakov, J. Genizi, O. Glazer, L. Yaniv, A. German, D. Miron, Y. Shachor-Meyouhas, E. Bamberger, K. Oved, T. M. Gottlieb, R. Navon, M. Paz, L. Etshtein, O. Boico, G. Kronenfeld, E. Eden, R. Cohen, H. Chappuy, F. Angoulvant, L. Lacroix and A. Gervaix, *Pediatrics*, 2017, **140**.

38. C. B. van Houten, J. A. H. de Groot, A. Klein, I. Srugo, I. Chistyakov, W. de Waal, C. B. Meijssen, W. Avis, T. F. W. Wolfs, Y. Shachor-Meyouhas, M. Stein, E. A. M. Sanders and L. J. Bont, *Lancet Infect. Dis.*, 2017, **17**, 431-440.

39. M. U. Bhuiyan, C. C. Blyth, R. West, J. Lang, T. Rahman, C. Granland, C. de Gier, M. L. Borland, R. B. Thornton, L. A. S. Kirkham, A. Martin, P. C. Richmond, D. W. Smith, A. Jaffe and T. L. Snelling, *Bmc Pulm Med*, 2019, **19**.

40. P. Venge, A.-K. Eriksson, S. Holmgren, L. Douhan-Håkansson, C. Peterson, S. Xu, S. Eriksson, D. Garwicz, A. Larsson and K. Pauksen, *J. Immunol. Methods* 2019, DOI: https://doi.org/10.1016/j.jim.2019.06.018.

41. A. Mayer-Scholl, P. Averhoff and A. Zychlinsky, *Curr. Opin. Microbiol.*, 2004, **7**, 62-66.

42. B. F. Rodak, George A. Fritsma and Elaine M. Keohane, *4th ed. St. Louis, Mo.: Elsevier Saunders, 2012. Print*, 2012.

43. X. Wang, G. Lin, G. Cui, X. Zhou and G. L. Liu, *Biosens. Bioelectron.*, 2017, **90**, 549-557.

44. T. Yusa, K. Tateda, A. Ohara and S. Miyazaki, *J. Infect.Chemother.*, 2017, **23**, 96-100.

45. S. L. Perkins, in *Wintrobe's Clinical Hematology*, ed. J. F. G. R. Lee, J. Lukens, F. Paraskevas, J. P. Greer and G. M. Rodgers, Lippincott Williams & Wilkins Philadelphia 10 edn., 1999, vol. 1, pp. 9-35.

46. M. L. Brigden, *Am Fam Physician*, 1999, **60**, 1443-1450.

47. C. Gabay and I. Kushner, *N. Engl. J. Med.*, 1999, **340**, 448-454.

48. L.-O. Hansson and L. Lindquist, *Curr. Opin. Infect. Dis.*, 1997, **10**, 196-201.

49. J. J. Morley and I. Kushner, *Ann. NY Acad. Sci.*, 1982, **389**, 406-418.

50. S. Noviello and D. B. Huang, *Diagnostics*, 2019, **9**, 37.

51. M. B. Pepys and G. M. Hirschfield, *J. Clin. Invest.*, 2003, **111**, 1805-1812.

52. L. Coelho, L. Rabello, J. Salluh, I. Martin-Loeches, A. Rodriguez, S. Nseir, J. A. Gomes and P. Povoa, *J. Crit. Care*, 2018, **48**, 385-389.

View Article Online
DOI: 10.1039/D0AN00896F

53. D. Coster, A. Wasserman, E. Fisher, O. Rogowski, D. Zeltser, I. Shapira, D. Bernstein, A. Meilik, E. Raykhshtat, P. Halpern, S. Berliner, S. Shenhar-Tsarfaty and R. Shamir, *Infection*, 2019, DOI: 10.1007/s15010-019-01383-6.
54. L. Marnell, C. Mold and T. W. Du Clos, *Clin. Immunol.*, 2005, **117**, 104-111.
55. C. Wacker, A. Prkno, F. M. Brunkhorst and P. Schlattmann, *Lancet Infect. Dis.*, 2013, **13**, 426-435.
56. S. Hammer, F. Meisner, C. Hammer and D. Seidel, *Transplant. Rev.*, 2000, **14**, 52-63.
57. J.-M. Zhang and J. An, *Int. Anesthesiol. Clin.*, 2007, **45**, 27.
58. E. Ferrero, P. Biswas, K. Vettoretto, M. Ferrarini, M. Uguccioni, L. Piali, B. E. Leone, B. Moser, C. Rugarli and R. Pardi, *Immunology*, 2003, **108**, 365-374.
59. J. Y. Hong, H. J. Lee, S. Y. Kim, K. S. Chung, E. Y. Kim, J. Y. Jung, M. S. Park, Y. S. Kim, S. K. Kim, J. Chang, S.-N. Cho and Y. A. Kang, *J. Infect.*, 2014, **68**, 252-258.
60. S. Kumar, S. Tripathy, A. Jyoti and S. G. Singh, *Biosens. Bioelectron.*, 2019, **124-125**, 205-215.
61. J. Angulo, C. Martinez-Valdebenito, C. Marco, H. Galeno, E. Villagra, L. Vera, N. Lagos, N. Becerra, J. Mora, A. Bermudez, J. Diaz, M. Ferres and M. Lopez-Lastra, *PLoS Negl. Trop. Dis.*, 2017, **11**.
62. A. V. Yamshchikov, N. S. Desai, H. M. Blumberg, T. R. Ziegler and V. Tangpricha, *Endocr Pract*, 2009, **15**, 438-449.
63. A. K. Zaas, T. Burke, M. Chen, M. McClain, B. Nicholson, T. Veldman, E. L. Tsalik, V. Fowler, E. P. Rivers, R. Otero, S. F. Kingsmore, D. Voora, J. Lucas, A. O. Hero, L. Carin, C. W. Woods and G. S. Ginsburg, *Sci. Transl. Med.*, 2013, **5**, 203ra126-203ra126.
64. S. Y. Zhou, X. W. Ren, J. Yang and Q. Jin, *Front. Microbiol.* , 2018, **9**.
65. D. L. Sampson, B. A. Fox, T. D. Yager, S. Bhide, S. Cermelli, L. C. McHugh, T. A. Seldon, R. A. Brandon, E. Sullivan, J. J. Zimmerman, M. Noursadeghi and R. B. Brandon, *Sci. Rep.*, 2017, **7**.
66. H. Melbye and N. Stocks, *Aust. Fam. Physician*, 2006, **35**, 513-517.
67. H. Melbye, D. Hvidsten, A. Holm, S. A. Nordbø and J. Brox, *Br. J. Gen. Pract.*, 2004, **54**, 653-658.
68. J. P. Herbeuval, A. Boasso, J. C. Grivel, A. W. Hardy, S. A. Anderson, M. J. Dolan, C. Chougnet, J. D. Lifson and G. M. Shearer, *Blood*, 2005, **105**, 2458-2464.
69. J. Sträter and P. Möller, in *Vitam. Horm.* , Academic Press, 2004, vol. 67, pp. 257-274.
70. K. Falconer, G. Askarieh, N. Weis, K. Hellstrand, A. Alaeus and M. Lagging, *Scand. J. Infect. Dis.*, 2010, **42**, 896-901.

View Article Online
DOI: 10.1039/D0AN00896F

71. M. G. Aabye, I. Latorre, J. Diaz, J. Maldonado, I. Mialdea, J. Eugen-Olsen, P. Ravn, J. Dominguez and M. Ruhwald, *Eur. Respir. .J.*, 2013, **42**, 495-503.
72. E. Eden, I. Srugo, T. Gottlieb, R. Navon, O. Boico, A. Cohen, E. Bamberger, A. Klein and K. Oved, *Journal of Infection*, 2016, **73**, 177-180.
73. T. Dong, S. Santos, Z. Yang, S. Yang and N. E. Kirkhus, *Analyst*, 2020, DOI: 10.1039/C9AN01704F.
74. P. Salvo, V. Dini, A. Kirchhain, A. Janowska, T. Oranges, A. Chiricozzi, T. Lomonaco, F. Di Francesco and M. Romanelli, *Sensors-Basel*, 2017, **17**, 2952.
75. W. N. Stassen, A. J. McCullough, B. R. Bacon, S. H. Gutnik, I. M. Wadiwala, C. McLaren, S. C. Kalhan and A. S. Tavill, *Gastroenterology*, 1986, **90**, 1247-1254.
76. P. E. Newburger and D. C. Dale, 2013.
77. N. Surana and D. Kasper, *Harrison's Principles of Internal Medicine. 20th ed. Access Medicine website. https://accessmedicine. mhmedical. com/content. aspx*, 2015.
78. P. Wetteland, M. Røger, H. Solberg and O. Iversen, *J. Intern. Med.*, 1996, **240**, 125-131.
79. C. Bray, L. N. Bell, H. Liang, R. Haykal, F. Kaiksow, J. J. Mazza and S. H. Yale, *WMJ*, 2016, **115**, 317-321.
80. M. B. Pepys and G. M. Hirschfield, *Journal of Clinical Investigation*, 2003, **111**, 1805-1812.
81. K. L. Becker, R. Snider and E. S. Nylen, *Crit. Care Med.*, 2008, **36**, 941-952.
82. K. Falconer, G. Askarieh, N. Weis, K. Hellstrand, A. Alaeus and M. Lagging, *Scandinavian Journal of Infectious Diseases*, 2010, **42**, 896-901.
83. L. Ashkenazi-Hoffnung, K. Oved, R. Navon, T. Friedman, O. Boico, M. Paz, G. Kronenfeld, L. Etshtein, A. Cohen, T. M. Gottlieb, E. Eden, I. Chistyakov, I. Srugo, A. Klein, S. Ashkenazi and O. Scheuerman, *Eur J Clin Microbiol*, 2018, **37**, 1361-1371.
84. K.-T. Liu, Y.-H. Liu, C.-Y. Lin, P.-L. Kuo and M.-C. Yen, *Exp. Ther. Med.*, 2016, **12**, 312-318.
85. B. A. Cunha, *Clin. Infect. Dis.*, 2004, **39**, 1260-1261.
86. M. Kandil, G. Khalil, E. El-Attar, G. Shehata and S. Hassan, *Braz. J. Microbiol. ,* 2018, **49**, 213-219.
87. I. Engelmann, F. Dubos, P.-E. Lobert, C. Houssin, V. Degas, A. Sardet, A. Decoster, A. Dewilde, A. Martinot and D. Hober, *Pediatrics*, 2015, **135**, e985-e993.
88. P. K. Sasidharan, E. Rajeev and V. Vijayakumari, *J. Assoc. Physicians India*, 2002, **50**, 554-558.
89. M. A. Sami, K. Wagner, P. Parikh and U. Hassan, 2019.
90. Z. T. F. Yu, J. G. Joseph, S. X. Liu, M. K. Cheung, P. J. Haffey, K. Kurabayashi and J. Fu, *Sens. Actuat. B Chem.*, 2017, **245**, 1050-1061.

View Article Online
DOI: 10.1039/D0AN00896F

91. C. Schulenburg, G. Faccio, D. Jankowska, K. Maniura-Weber and M. Richter, *Analyst*, 2016, **141**, 1645-1648.
92. E. Ng, C. Yao, T. O. Shultz, S. Ross-Howe and S. X. Wang, *Nanomed: Nanotechnol.*, 2019, **16**, 10-19.
93. Chun, T. D. Chung and H. C. Kim, *Anal. Chem.*, 2005, **77**, 2490-2495.
94. A. Zhbanov and S. Yang, *Anal Methods-Uk*, 2018, **10**, 180-189.
95. W. Miao and A. J. Bard, *Anal. Chem.*, 2003, **75**, 5825-5834.
96. Z. Yang, Y. Liu, C. Lei, X.-c. Sun and Y. Zhou, *Microchim. Acta*, 2015, **182**, 2411-2417.
97. D. Martens, P. Ramirez-Priego, M. S. Murib, A. A. Elamin, A. B. Gonzalez-Guerrero, M. Stehr, F. Jonas, B. Anton, N. Hlawatsch, P. Soetaert, R. Vos, A. Stassen, S. Severi, W. Van Roy, R. Bockstaele, H. Becker, M. Singh, L. M. Lechuga and P. Bienstman, *Anal Methods-Uk*, 2018, **10**, 3066-3073.
98. J. D. McBride and M. A. Cooper, *J. Nanobiotechnol.*, 2008, **6**, 5.
99. T. Goda, M. Toya, A. Matsumoto and Y. Miyahara, *ACS Appl. Mater.*, 2015, **7**, 27440-27448.
100. A. S. Tanak, B. Jagannath, Y. Tamrakar, S. Muthukumar and S. Prasad, *Anal. Chim. Acta*, 2019, **3**, 100029.
101. A. Belushkin, F. Yesilkoy and H. Altug, *ACS Nano*, 2018, **12**, 4453-4461.
102. N. Fabri-Faja, O. Calvo-Lozano, P. Dey, R. A. Terborg, M. C. Estevez, A. Belushkin, F. Yesilköy, L. Duempelmann, H. Altug, V. Pruneri and L. M. Lechuga, *Anal. Chim. Acta*, 2019, **1077**, 232-242.
103. Á. Molinero-Fernández, M. Moreno-Guzmán, L. Arruza, M. Á. López and A. Escarpa, *ACS Sens.*, 2019, **4**, 2117-2123.
104. J. M. Lim, M. Y. Ryu, J. H. Kim, C. H. Cho, T. J. Park and J. P. Park, *RSC Adv.*, 2017, **7**, 36562-36565.
105. V. Kamakoti, D. Kinnamon, K. H. Choi, B. Jagannath and S. Prasad, *Future Sci. OA*, 2018, **4**.
106. S. M. R. Alejandra Alba-Patiño , Marcio Borges , Nicolas Pazos-Perez , Ramon A Alvarez-Puebla and Roberto de la Rica, *Nanoscale Adv.*, 2020, DOI: 10.1039/D0NA00026D Accepted Manuscript.
107. C. X. Liu, H. Y. Cai, J. Jia, T. Y. Cao, Y. Li, J. H. Sun, C. H. Xu and C. Liu, *Int Conf Nano Micro*, 2017, 784-787.
108. Z. H. Ibupoto, N. Jamal, K. Khun and M. Willander, *Sens. Actuat. B Chem.*, 2012, **166-167**, 809-814.
109. T. Bryan, X. Luo, P. R. Bueno and J. J. Davis, *Biosens. Bioelectron.*, 2013, **39**, 94-98.
110. M. S. Islam, H. Yu, H. G. Lee and S. H. Kang, *Biosens. Bioelectron.*, 2010, **26**, 1028-1035.

View Article Online
DOI: 10.1039/D0AN00896F

111. C. R. Zamarreño, I. Ardaiz, L. Ruete, F. J. Muñoz, I. R. Matias and F. J. Arregui, 2013.
112. B. B. Kim, W. J. Im, J. Y. Byun, H. M. Kim, M.-G. Kim and Y.-B. Shin, *Sens. Actuat. B Chem.*, 2014, **190**, 243-248.
113. J. Hu, Z.-L. Zhang, C.-Y. Wen, M. Tang, L.-L. Wu, C. Liu, L. Zhu and D.-W. Pang, *Anal. Chem.*, 2016, **88**, 6577-6584.
114. M. H. F. Meyer, M. Hartmann and M. Keusgen, *Biosens. Bioelectron.*, 2006, **21**, 1987-1990.
115. Y. Kitayama and T. Takeuchi, *Anal. Chem.*, 2014, **86**, 5587-5594.
116. P. Buchegger, U. Sauer, H. Toth-Szekely and C. Preininger, *Sensors-Basel*, 2012, **12**, 1494-1508.
117. S.-W. Kim, I.-H. Cho, G.-S. Lim, G.-N. Park and S.-H. Paek, *Biosens. Bioelectron.*, 2017, **98**, 7-14.
118. C.-H. Kim, J.-H. Ahn, J.-Y. Kim, J.-M. Choi, K.-C. Lim, T. Jung Park, N. Su Heo, H. Gu Lee, J.-W. Kim and Y.-K. Choi, *Biosens. Bioelectron.*, 2013, **41**, 322-327.
119. B. Esteban-Fernández de Ávila, V. Escamilla-Gómez, S. Campuzano, M. Pedrero, J. P. Salvador, M. P. Marco and J. M. Pingarrón, *Sens. Actuat. B Chem.*, 2013, **188**, 212-220.
120. S. K. Vashist, E. Marion Schneider, R. Zengerle, F. von Stetten and J. H. T. Luong, *Biosens. Bioelectron.*, 2015, **66**, 169-176.
121. D. Rascher, A. Geerlof, E. Kremmer, P. Krämer, M. Schmid, A. Hartmann and M. Rieger, *Biosens. Bioelectron.*, 2014, **59**, 251-258.
122. G. Sener, E. Ozgur, A. Y. Rad, L. Uzun, R. Say and A. Denizli, *Analyst*, 2013, **138**, 6422-6428.
123. S. K. Vashist, E. M. Schneider, E. Barth and J. H. T. Luong, *Anal. Chim. Acta*, 2016, **938**, 129-136.
124. Z.-H. Yang, S. Ren, Y. Zhuo, R. Yuan and Y.-Q. Chai, *Anal.Chem.*, 2017, **89**, 13349-13356.
125. A. Liu and X. Wang, *Int. J. Electrochem.*, 2015, **10**, 9342-9350.
126. Z. Yang, Y. Liu, C. Lei, X.-c. Sun and Y. Zhou, *Microchim. Acta*, 2015, **182**, 2411-2417.
127. H. Li, Y. Sun, J. Elseviers, S. Muyldermans, S. Liu and Y. Wan, *Analyst*, 2014, **139**, 3718-3721.
128. A. Panneer Selvam and S. Prasad, *SLAS Technol.*, 2017, **22**, 338-347.
129. P. Liu, C. Li, R. Zhang, Q. Tang, J. Wei, Y. Lu and P. Shen, *Biosens. Bioelectron.*, 2019, **126**, 543-550.
130. C.-Y. Chiang, T.-T. Huang, C.-H. Wang, C.-J. Huang, T.-H. Tsai, S.-N. Yu, Y.-T. Chen, S.-W. Hong, C.-W. Hsu, T.-C. Chang and L.-K. Chau, *Biosens. Bioelectron.*, 2020, **151**, 111871.
131. P. Chen, M. T. Chung, W. McHugh, R. Nidetz, Y. Li, J. Fu, T. T. Cornell, T. P. Shanley and K. Kurabayashi, *ACS Nano*, 2015, **9**, 4173-4181.
132. *Japan Pat.*, US9334477B2, 2016.

View Article Online
DOI: 10.1039/D0AN00896F

133. Q. Fu, Z. Wu, J. Li, Z. Wu, H. Zhong, Q. Yang, Q. Liu, Z. Liu, L. Sheng, M. Xu, T. Li, Z. Yin and Y. Wu, *J. Nanobiotechnol.*, 2019, **17**, 67.
134. A. Furniturewalla, M. Chan, J. Sui, K. Ahuja and M. Javanmard, *Microsyst. Nanoeng.*, 2018, **4**, 20.
135. S. Zhang, Z. Li and Q. Wei, *Precis. Eng.*, 2020, DOI: https://doi.org/10.1016/j.npe.2019.12.004.
136. H. C. Sox and M. H. Liang, *Annal. of Internal Medicine*, 1986, **104**, 515-523.
137. Y. Liu, Z. Matharu, A. Rahimian and A. Revzin, *Biosens. Bioelectron.*, 2015, **64**, 43-50.
138. A. H. Agbaria, G. Beck Rosen, I. Lapidot, D. H. Rich, M. Huleihel, S. Mordechai, A. Salman and J. Kapelushnik, *Analytical Chemistry*, 2018, **90**, 7888-7895.
139. U. Zelig, S. Mordechai, G. Shubinsky, R. K. Sahu, M. Huleihel, E. Leibovitz, I. Nathan and J. Kapelushnik, *Biochimica et Biophysica Acta (BBA)-General Subjects*, 2011, **1810**, 827-835.
140. A. H. Agbaria, G. B. Rosen, I. Lapidot, D. H. Rich, S. Mordechai, J. Kapelushnik, M. Huleihel and A. Salman, *Journal of Biophotonics*, 2020, **13**, e201900215.

View Article Online
DOI: 10.1039/D0AN00896F

Table of content

Schematic diagram showing multiple modes of biosensing platforms for diagnosis of bacterial or viral infections

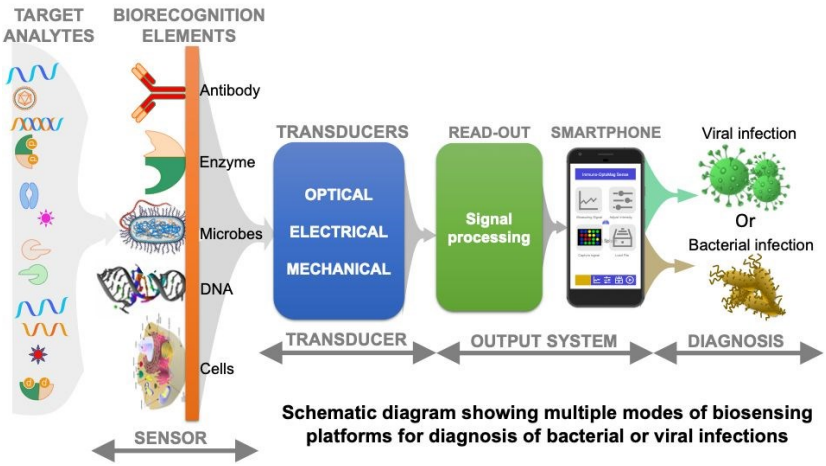

Schematic diagram showing multiple modes of biosensing platforms for diagnosis of bacterial or viral infections